NACA TN 2621

NATIONAL ADVISORY COMMITTEE FOR AERONAUTICS

TECHNICAL NOTE 2621

DEFLECTION AND STRESS ANALYSIS OF THIN SOLID WINGS OF ARBITRARY PLAN FORM WITH PARTICULAR REFERENCE TO DELTA WINGS

By Manuel Stein, J. Edward Anderson, and John M. Hedgepeth

Langley Aeronautical Laboratory
Langley Field, Va.

NACA

Washington

February 1952

1T

NATIONAL ADVISORY COMMITTEE FOR AERONAUTICS

TECHNICAL NOTE 2621

DEFLECTION AND STRESS ANALYSIS OF THIN SOLID WINGS OF ARBITRARY PLAN FORM WITH PARTICULAR REFERENCE TO DELTA WINGS

By Manuel Stein, J. Edward Anderson,
and John M. Hedgepeth

SUMMARY

The structural analysis of arbitrary solid cantilever wings by small-deflection thin-plate theory is reduced to the solution of linear ordinary differential equations by the assumption that the chordwise deflections at any spanwise station may be expressed in the form of a power series in which the coefficients are functions of the spanwise coordinate. If the series is limited to the first two and three terms (that is, if linear and parabolic chordwise deflections, respectively, are assumed), the differential equations for the coefficients are solved exactly for uniformly loaded solid delta wings of constant thickness and of diamond chordwise cross section with constant thickness ratio. For cases for which exact solutions to the differential equations cannot be obtained, a numerical procedure is derived. Experimental deflection and stress data for constant-thickness delta-plate specimens of 45° and 60° sweep are presented and are found to compare favorably with the present theory.

INTRODUCTION

One of the present trends in the development of high-speed airplanes and missiles is toward the use of thin low-aspect-ratio wings. The structural analysis of these wings often cannot be based on beam theory since the structural deformations may vary considerably from those of a beam and, indeed, may more closely approach those of a plate. In cases where the wing construction is solid or nearly solid the use of plate theory in the analysis is particularly valid, and it is this type of wing which is considered in the present paper.

Exact solutions to the partial-differential equation of plate theory are not readily obtained, especially for plates of arbitrary shape and loading; however, a number of approximate solutions to

specific problems on cantilever plates have appeared in the literature (see, for example, references 1 to 7). Of the approaches used in these references, only the one in references 6 and 7 is readily applicable to plates of arbitrary plan form, thickness distribution, and load distribution; thus it is the most useful one for the analysis of actual wings.

In reference 6 the cantilever-plate problem is simplified by the assumption that the deformations of the plate in the chordwise direction (parallel to the root) are linear. By minimizing the potential energy of the plate, the partial-differential equation of plate theory is replaced by two simultaneous ordinary differential equations for the spanwise variations of the bending deflection and twist. In reference 7 the same ordinary differential equations are obtained in a different manner. Refinement of the analysis by inclusion of the effect of parabolic, cubic, or higher-order chordwise camber terms is indicated in reference 6, and as the order of refinement is increased a corresponding increase in the number of ordinary differential equations is obtained.

In the present paper, which is an extension of reference 6, a general set of ordinary differential equations is presented which may be used to obtain any desired degree of approximation to the deflection of the plate. These equations are solved exactly for several cases of delta plates under uniform load first by considering linear chordwise deformation only and second by including the effect of parabolic chordwise camber. Comparisons are drawn between the stresses and deflections computed from the equations of each approximation and also with some experimental results.

The differential equations presented contain coefficients that depend on the plan form and stiffness distribution of the plate and on the loading. In the present paper, the plates considered in detail have coefficients such that the differential equations can be solved exactly; however, in cases for which exact solutions cannot be obtained a numerical procedure must be used. One such procedure is derived and its accuracy is demonstrated.

SYMBOLS

l	length of plate measured perpendicular to root
c	root chord of plate
p	lateral load per unit area, positive in z-direction

t	local thickness of plate
t_{av}	average thickness of plate
D	local flexural stiffness $\left(\frac{Et^3}{12(1-\mu^2)}\right)$
$\overline{D}$	flexural stiffness based on average thickness $\left(\frac{Et_{av}^3}{12(1-\mu^2)}\right)$
E	modulus of elasticity of material
μ	Poisson's ratio
w	deflection of plate, positive in z-direction
x,y,z	coordinates defined in figure 1
φ_n	function of x, coefficient in power series for deflection $w = \sum_{n=0}^{N} \varphi_n(x)y^n$
$c_1(x),c_2(x)$	functions defining plan form (see fig. 1)
x_1	variable obtained by transformation $x_1 = 1 - \frac{x}{l}$
σ_x,σ_y	normal stresses
τ_{xy}	shear stress
σ	maximum principal stress
λ	aspect-ratio parameter $\left(\frac{l}{c}\sqrt{\frac{3}{2}(1-\mu)}\right)$

RESULTS

The derivation of the general set of ordinary differential equations is given in appendix A. The general procedure outlined in reference 6 is followed; that is, the deflection of the plate w is expanded into a power series in y the chordwise coordinate, with

coefficients which are functions of x the spanwise coordinate (see fig. 1)

$$w = \varphi_0(x) + \varphi_1(x)y + \varphi_2(x)y^2 + \ldots + \varphi_N(x)y^N \qquad (1)$$

Equation (1) is substituted into the expression for the potential energy of the plate-load combination which is in turn minimized by the calculus of variations with respect to each of the coefficients φ_n. The results of the variational procedure appear as $N + 1$ simultaneous differential equations with the coefficients φ_n as unknowns.

By taking a sufficient number of terms in the expansion of w, the resulting differential equations can be used to obtain any desired degree of accuracy in the solution for the deflections of any given cantilever plate subjected to an arbitrary lateral load. Of most interest, perhaps, are the particular cases for $N = 1$ and $N = 2$, which are obtained from the general set of equations and are simplified in appendix A. The case for $N = 1$ (also derived in references 6 and 7) includes linear chordwise deflections, and the case for $N = 2$ takes into account parabolic chordwise curvature. Although for most practical problems the solution by the parabolic theory should be adequate, cases might exist in which cubic, quartic, or even higher-order chordwise terms should be included, depending on the convergence of the series for the configuration considered.

The particular equations for $N = 1$ and $N = 2$ are used to determine the deflections and stresses of the following cantilever plates subjected to uniform lateral load:

(1) A 45° delta plate of uniform thickness

(2) A 60° delta plate of uniform thickness

(3) A 45° delta plate of diamond chordwise cross section with constant thickness ratio

Fortunately, for these configurations, the solution can be carried out exactly by both the linear and parabolic theories, and the details of these exact solutions are included in appendix B. In general, however, exact solutions cannot be obtained and some numerical method must be used. One such method, based on replacing derivatives by their first-order-approximation difference forms, is derived in appendix C.

A summary of the results for the three particular problems is shown in figures 2 to 11. Deflections obtained by the linear theory and the parabolic theory for the three configurations are compared in figures 2, 3, and 4.

Stresses obtained by the linear theory and the parabolic theory for the three configurations are compared in figures 5, 6, and 7. Where available, experimental deflections and stresses are also shown in these figures. The details of the procedure used to obtain the experimental deflections of the 45° and 60° uniform-thickness plates and the experimental stresses in the 45° uniform-thickness plate are contained in appendix D; whereas the experimental root stresses for the 60° uniform-thickness plate were obtained from reference 8. Figures 8 to 11 present the comparison between deflections and stresses computed from the exact solutions of the differential equations and those computed from the numerical solution of the same equations.

DISCUSSION

The results shown in figures 2 and 3 indicate that, with regard to deflections, either the linear theory or the parabolic theory is adequate for the case of a constant-thickness delta plate subjected to a uniform load, the comparison being somewhat better for the 60° plate than for the 45° plate. If accurate slopes in the chordwise direction (angle of attack) are desired, however, the parabolic theory must be used because the error in the angle of attack as computed by the linear theory is as much as 30 percent (see figs. 2 and 3). The appreciable anticlastic curvature, evidenced by the experimental results of figures 2 and 3, may be important aerodynamically and is, of course, not taken into account by the linear theory.

The apparent convergence of the aforementioned series in the case of the diamond-cross-section plate (see fig. 4) implies that the linear theory is adequate for this case. The lack of chordwise curvature in the result obtained by the parabolic theory is attributable to the fact that the natural tendency of the plate to have anticlastic curvature is canceled by the opposite tendency of the thin edges to bend down under the load. Unfortunately, no experimental results are available for this configuration.

In figure 4 the plate stiffness $\bar{D}$ in the nondimensional parameter $w\bar{D}/pl^4$ is the local value of D at a point where the thickness is equal to the average thickness of the plate as a whole. Thus the results of figure 4 are comparable with the results of figure 2 on an equal-weight basis. It can be seen that the deflections of the diamond-cross-section, constant-thickness-ratio plate are everywhere less than those of the uniform-thickness plate although they increase rapidly near the tip. This curling-up or singularity in slope at the tip is a result of using a small-deflection theory and probably would not be so marked in an actual case.

The stress results for the 45° and 60° uniform-thickness delta plates indicate that both the linear and the parabolic theories are adequate and that the parabolic theory is better than the linear theory only near the root. It should be noted that, although the maximum principal stress over a large part of the 45° plate is plotted in figure 5, only the stresses normal to the root along the line $\frac{x}{l} = 0.0087$ of the 60° plate are plotted in figure 6 since only these stresses are given in reference 8. (The maximum principal stress and the stress normal to the root are theoretically equal at the root since the root shear stress is zero.)

Experimental data are lacking for the diamond-cross-section delta plate and, therefore, only theoretical stresses are shown in figure 7. As in the case of deflections, the results obtained from the linear theory and those obtained from the parabolic theory are almost coincident, the difference being greatest near the root. Figure 7 has also been plotted so that the results are directly comparable with those for the 45° uniform-thickness plate in figure 5 on an equal-weight basis. As can be expected, the diamond-cross-section, constant-thickness-ratio plate is a better design structurally; the stresses in the diamond-cross-section plate are everywhere smaller and are almost constant in the spanwise direction.

The theoretical results in figures 2 to 7 have been obtained from exact solutions of the differential equations of the linear and parabolic theories. In order to test the reliability of the numerical method derived in appendix C, the differential equations were also solved numerically. The results shown in figures 8 and 9 indicate that the agreement is good between the numerical solution in which five equal intervals were used and the exact solution of the differential equations for the case of the 45° uniform-thickness plate. The same good agreement can be expected in other cases where the thickness and load distributions are not too erratic and where the plate stiffness does not go to zero at the tip; that is, when no signularities appear at the tip.

Since the efficacy of the numerical method depends on how well parabolic arcs fit the various functions between stations, serious error can result from blind application. An example of the seriousness of these errors and of the manner in which they can be remedied is shown in figures 10 and 11. In these figures a comparison is made between exact and numerical results obtained on the 45° diamond-cross-section, constant-thickness-ratio plate. As can be expected, the five-station numerical solution fails to follow the exact solution in the neighborhood of the singularity at the tip. Since the region of trouble is localized at the tip, a reasonable remedy would be to decrease the spacing of the station points near the tip. This decrease in spacing may be accomplished either by using a greater number of equally spaced

stations or by using unequally spaced stations crowded near the tip. The increase in accuracy obtained by increasing the number of equally spaced station points to ten is shown in figures 10 and 11.

CONCLUDING REMARKS

The general method presented herein for finding deflections and stresses of solid or nearly solid wings is, in principle, capable of yielding arbitrarily accurate results for any configuration. It is seen that, for the examples considered, only the first two or three terms in the series expansion need be considered to obtain adequate accuracy. In addition, for most practical plate-like wings with clamped roots the first two or three terms will probably be adequate, although problems may exist wherein more terms are needed.

The numerical procedure, derived for application in cases where exact solutions cannot be obtained, gives good agreement when compared with exact solutions if enough stations are taken along the span. The necessary number of stations is dependent on the type of thickness and loading distribution considered, five equally spaced stations being enough for the uniform-thickness delta wing subjected to uniform loading, and ten being necessary for the diamond-cross-section, constant-thickness-ratio delta wing subjected to uniform loading.

Langley Aeronautical Laboratory
National Advisory Committee for Aeronautics
Langley Field, Va., November 30, 1951

APPENDIX A

DERIVATION OF DIFFERENTIAL EQUATIONS

The structure considered herein is a thin, elastic, isotropic, cantilever plate of arbitrary plan form and slowly varying thickness subjected to distributed lateral load (see fig. 1). By assuming that the deflection of the plate can be represented by a power series in the chordwise coordinate and by applying the minimum-potential-energy principle, a set of ordinary differential equations in the spanwise coordinate is obtained from which the coefficients of the power series may be determined. First the general set of equations is derived; then the particular equations for the cases of linear chordwise deflections and parabolic chordwise deflections are deduced from the general set and simplified.

General equations.- The potential energy of the system under consideration is

$$\text{Potential energy} = \int_0^l \int_{c_1(x)}^{c_2(x)} \left\{ \frac{D(x,y)}{2} \left[\left(\frac{\partial^2 w}{\partial x^2} \right)^2 + \left(\frac{\partial^2 w}{\partial y^2} \right)^2 + 2\mu \frac{\partial^2 w}{\partial x^2} \frac{\partial^2 w}{\partial y^2} + 2(1 - \mu) \left(\frac{\partial^2 w}{\partial x \, \partial y} \right)^2 \right] - p(x,y)w \right\} dy \, dx \tag{A1}$$

in which

$$D(x,y) = \frac{E\left[t(x,y)\right]^3}{12(1 - \mu^2)}$$

and $p(x,y)$ is the distributed lateral load.

The assumption is made that the deflection w can be represented by the power series

$$w = \sum_{n=0}^{N} \varphi_n(x) y^n \tag{A2}$$

Substitution of this expression for w into equation (A1) gives

$$\text{Potential energy} = \int_0^l dx \left\{ \frac{1}{2} \sum_{m=0}^{N} \sum_{n=0}^{N} \left[a_{m+n+1} \varphi_m'' \varphi_n'' + mn(m-1)(n-1) a_{m+n-3} \varphi_m \varphi_n + 2\mu n(n-1) a_{m+n-1} \varphi_m'' \varphi_n + 2(1-\mu) mn a_{m+n-1} \varphi_m' \varphi_n' \right] - \sum_{n=0}^{N} p_{n+1} \varphi_n \right\} \tag{A3}$$

in which

$$\left.\begin{aligned} a_r &= \int_{c_1(x)}^{c_2(x)} D(x,y) y^{r-1} dy \qquad (r = 1, 2, \ldots 2N+1) \\ p_r &= \int_{c_1(x)}^{c_2(x)} p(x,y) y^{r-1} dy \qquad (r = 1, 2, \ldots N+1) \end{aligned}\right\} \tag{A4}$$

and the primes denote differentiation with respect to x.

Minimization of the potential energy by means of the calculus of variations gives

$$\delta(\text{Potential energy}) = 0$$

$$= \int_0^l dx \left\{ \frac{1}{2} \sum_{m=0}^{N} \sum_{n=0}^{N} \left[a_{m+n+1} \left(\varphi_m'' \delta\varphi_n'' + \varphi_n'' \delta\varphi_m'' \right) + mn(m-1)(n-1) a_{m+n-3} \left(\varphi_m \delta\varphi_n + \varphi_n \delta\varphi_m \right) + 2\mu n(n-1) a_{m+n-1} \left(\varphi_m'' \delta\varphi_n + \varphi_n \delta\varphi_m'' \right) + 2(1-\mu) mn a_{m+n-1} \left(\varphi_m' \delta\varphi_n' + \varphi_n' \delta\varphi_m' \right) \right] - \sum_{n=0}^{N} p_{n+1} \delta\varphi_n \right\}$$

Integrating by parts and collecting terms results in

$$0 = \int_0^l dx \sum_{n=0}^{N} \delta\varphi_n \left\{ \sum_{m=0}^{N} \left[\left(a_{m+n+1}\varphi_m'' \right)'' + \mu m(m-1)\left(a_{m+n-1}\varphi_m \right)'' - 2(1-\mu)mn\left(a_{m+n-1}\varphi_m' \right)' + \mu n(n-1) a_{m+n-1}\varphi_m'' + mn(m-1)(n-1) a_{m+n-3}\varphi_m \right] - p_{n+1} \right\} + \left\{ \sum_{n=0}^{N} \delta\varphi_n' \sum_{m=0}^{N} \left[a_{m+n+1}\varphi_m'' + \mu m(m-1) a_{m+n-1}\varphi_m \right] \right\}_0^l - \left\{ \sum_{n=0}^{N} \delta\varphi_n \sum_{m=0}^{N} \left[\left(a_{m+n+1}\varphi_m'' \right)' + \mu m(m-1)\left(a_{m+n-1}\varphi_m \right)' - 2(1-\mu)mn a_{m+n-1}\varphi_m' \right] \right\}_0^l \qquad (A5)$$

Everywhere in the region of the plate, except at the boundary $x = 0$, the variation of w is arbitrary. At $x = 0$ the cantilever boundary conditions

$$w = \frac{\partial w}{\partial x} = 0$$

yield

$$\varphi_n(0) = \varphi_n'(0) = 0 \qquad (n = 0, 1, \ldots N) \qquad (A6)$$

and therefore the variation in these quantities must also be zero at $x = 0$.

Equation (A5) is then satisfied if, in addition to equation (A6),

$$\sum_{m=0}^{N} \left[\left(a_{m+n+1}\varphi_m'' \right)'' + \mu m(m-1)\left(a_{m+n-1}\varphi_m \right)'' - 2(1-\mu)mn\left(a_{m+n-1}\varphi_m' \right)' + \mu n(n-1) a_{m+n-1}\varphi_m'' + mn(m-1)(n-1) a_{m+n-3}\varphi_m \right] = p_{n+1}$$

$$(n = 0, 1, \ldots N) \qquad (A7)$$

$$\sum_{m=0}^{N} \left[a_{m+n+1}\varphi_m'' + \mu m(m-1) a_{m+n-1}\varphi_m \right]_{x=l} = 0 \qquad (n = 0, 1, \ldots N) \qquad (A8)$$

and

$$\sum_{m=0}^{N}\left[\left(a_{m+n+1}\varphi_m''\right)' + \mu m(m-1)\left(a_{m+n-1}\varphi_m\right)' - 2(1-\mu)mna_{m+n-1}\varphi_m'\right]_{x=l} = 0$$

$$(n = 0, 1, \ldots N) \quad \text{(A9)}$$

Equations (A7) form a set of $N + 1$ simultaneous ordinary differential equations for the functions $\varphi_n(x)$. The functions φ_n are completely determined by these differential equations and the boundary conditions (A6), (A8), and (A9).

Particular case of linear chordwise deflections.- If $N = 1$, the deflection function becomes

$$w = \varphi_0 + y\varphi_1 \quad \text{(A10)}$$

a linear function in the chordwise direction, where φ_0 is the bending deflection and φ_1 is the twist. Equations (A7) become

$$\left(a_1\varphi_0''\right)'' + \left(a_2\varphi_1''\right)'' = p_1 \quad \text{(A11)}$$

$$\left(a_2\varphi_0''\right)'' + \left(a_3\varphi_1''\right)'' - 2(1-\mu)\left(a_1\varphi_1'\right)' = p_2 \quad \text{(A12)}$$

The root boundary conditions, given by equation (A6), become

$$\varphi_0(0) = \varphi_0'(0) = \varphi_1(0) = \varphi_1'(0) = 0 \quad \text{(A13)}$$

The tip boundary conditions, given by equations (A8) and (A9), become

$$\left(a_1\varphi_0'' + a_2\varphi_1''\right)_{x=l} = 0 \quad \text{(A14)}$$

$$\left(a_2\varphi_0'' + a_3\varphi_1''\right)_{x=l} = 0 \quad \text{(A15)}$$

$$\left[\left(a_1\varphi_0''\right)' + \left(a_2\varphi_1''\right)'\right]_{x=l} = 0 \quad \text{(A16)}$$

$$\left[\left(a_2\varphi_0''\right)' + \left(a_3\varphi_1''\right)' - 2(1-\mu)a_1\varphi_1'\right]_{x=l} = 0 \qquad \text{(A17)}$$

Equations (A11) to (A17) are the differential equations and corresponding boundary conditions presented in reference 6 (if only distributed load is considered) where the symbols W and θ are used instead of φ_0 and φ_1, respectively.

If equation (A11) is integrated twice and the boundary conditions (A14) and (A16) are used,

$$\varphi_0'' = -\frac{a_2}{a_1}\varphi_1'' + \frac{1}{a_1}\int_x^l \int_x^l p_1 \, dx^2 \qquad \text{(A18)}$$

Substitution of φ_0'' into equations (A12), (A15), and (A17) gives

$$\left(b_1\varphi_1''\right)'' - 2(1-\mu)\left(a_1\varphi_1'\right)' = p_2 - \left(\frac{a_2}{a_1}\int_x^l \int_x^l p_1 \, dx^2\right)'' \qquad \text{(A19)}$$

$$\left(b_1\varphi_1''\right)_{x=l} = 0 \qquad \text{(A20)}$$

$$\left[\left(b_1\varphi_1''\right)' - 2(1-\mu)a_1\varphi_1'\right]_{x=l} = 0 \qquad \text{(A21)}$$

in which

$$b_1 = a_3 - \frac{a_2^2}{a_1}$$

If equation (A19) is integrated once and the boundary condition (A21) is used,

$$\left(b_1\varphi_1''\right)' - 2(1-\mu)a_1\varphi_1' = -\int_x^l p_2 \, dx - \left(\frac{a_2}{a_1}\int_x^l \int_x^l p_1 \, dx^2\right)' \qquad \text{(A22)}$$

The differential equation (A22) is a second-order differential equation in φ_1'. The twist φ_1 and then the bending deflection φ_0 are obtained by solving equations (A22) and (A18), respectively, by applying the boundary conditions (A13) and (A20).

Particular case of parabolic chordwise deflections.- The effect of parabolic chordwise camber may be included by letting $N = 2$ in the general power series (equation (A2)). If $N = 2$ the deflection function becomes

$$w = \varphi_0 + y\varphi_1 + y^2\varphi_2$$

Here φ_2 represents the spanwise distribution of parabolic chordwise camber. For this case the differential equations (A7) become

$$\left(a_1\varphi_0''\right)'' + \left(a_2\varphi_1''\right)'' + \left(a_3\varphi_2''\right)'' + 2\mu\left(a_1\varphi_2\right)'' = p_1 \tag{A23}$$

$$\left(a_2\varphi_0''\right)'' + \left(a_3\varphi_1''\right)'' + \left(a_4\varphi_2''\right)'' + 2\mu\left(a_2\varphi_2\right)'' - 2(1 - \mu)\left[\left(a_1\varphi_1'\right)' + 2\left(a_2\varphi_2'\right)'\right] = p_2 \tag{A24}$$

$$\left(a_3\varphi_0''\right)'' + \left(a_4\varphi_1''\right)'' + \left(a_5\varphi_2''\right)'' + 2\mu\left[a_1\varphi_0'' + a_2\varphi_1'' + a_3\varphi_2'' + \left(a_3\varphi_2\right)''\right] - 4(1 - \mu)\left[\left(a_2\varphi_1'\right)' + 2\left(a_3\varphi_2'\right)'\right] + 4a_1\varphi_2 = p_3 \tag{A25}$$

with the boundary conditions

$$\varphi_0(0) = \varphi_0'(0) = \varphi_1(0) = \varphi_1'(0) = \varphi_2(0) = \varphi_2'(0) = 0 \tag{A26}$$

$$\left(a_1\varphi_0'' + a_2\varphi_1'' + a_3\varphi_2'' + 2\mu a_1\varphi_2\right)_{x=l} = 0 \tag{A27}$$

$$\left(a_2\varphi_0'' + a_3\varphi_1'' + a_4\varphi_2'' + 2\mu a_2\varphi_2\right)_{x=l} = 0 \tag{A28}$$

$$\left(a_3\varphi_0'' + a_4\varphi_1'' + a_5\varphi_2'' + 2\mu a_3\varphi_2\right)_{x=l} = 0 \tag{A29}$$

$$\left[\left(a_1\varphi_0''\right)' + \left(a_2\varphi_1''\right)' + \left(a_3\varphi_2''\right)' + 2\mu\left(a_1\varphi_2\right)'\right]_{x=l} = 0 \tag{A30}$$

$$\left[\left(a_2\varphi_0''\right)' + \left(a_3\varphi_1''\right)' + \left(a_4\varphi_2''\right)' + 2\mu\left(a_2\varphi_2\right)' - 2(1 - \mu)\left(a_1\varphi_1' + 2a_2\varphi_2'\right)\right]_{x=l} = 0 \tag{A31}$$

$$\left[\left(a_3\varphi_0''\right)' + \left(a_4\varphi_1''\right)' + \left(a_5\varphi_2''\right)' + 2\mu\left(a_3\varphi_2\right)' - 4(1 - \mu)\left(a_2\varphi_1' + 2a_3\varphi_2'\right)\right]_{x=l} = 0 \tag{A32}$$

If equation (A23) is integrated twice and the boundary conditions (A27) and (A30) are used,

$$\varphi_0'' = -\frac{a_2}{a_1}\varphi_1'' - \frac{a_3}{a_1}\varphi_2'' - 2\mu\varphi_2 + \frac{1}{a_1}\int_x^l\int_x^l p_1\,dx^2 \tag{A33}$$

Substitution of φ_0'' into the remaining differential equations and boundary conditions results in

$$\left(b_1\varphi_1''\right)'' + \left(b_2\varphi_2''\right)'' - 2(1 - \mu)\left[\left(a_1\varphi_1'\right)' + 2\left(a_2\varphi_2'\right)'\right] = p_2 - \left(\frac{a_2}{a_1}\int_x^l\int_x^l p_1\,dx^2\right)'' \tag{A34}$$

$$\left(b_2\varphi_1''\right)'' + \left(b_3\varphi_2''\right)'' - 4(1 - \mu)\left[\left(a_2\varphi_1'\right)' + 2\left(a_3\varphi_2'\right)'\right] + 4\left(1 - \mu^2\right)a_1\varphi_2 = p_3 - 2\mu\int_x^l\int_x^l p_1\,dx^2 - \left(\frac{a_3}{a_1}\int_x^l\int_x^l p_1\,dx^2\right)'' \tag{A35}$$

$$\left(b_1\varphi_1'' + b_2\varphi_2''\right)_{x=l} = 0 \tag{A36}$$

$$\left[\left(b_1\varphi_1''\right)' + \left(b_2\varphi_2''\right)' - 2(1-\mu)\left(a_1\varphi_1' + 2a_2\varphi_2'\right)\right]_{x=l} = 0 \qquad \text{(A37)}$$

$$\left(b_2\varphi_1'' + b_3\varphi_2''\right)_{x=l} = 0 \qquad \text{(A38)}$$

$$\left[\left(b_2\varphi_1''\right)' + \left(b_3\varphi_2''\right)' - 4(1-\mu)\left(a_2\varphi_1' + 2a_3\varphi_2'\right)\right]_{x=l} = 0 \qquad \text{(A39)}$$

$$\varphi_1(0) = \varphi_1'(0) = \varphi_2(0) = \varphi_2'(0) = 0 \qquad \text{(A40)}$$

in which

$$b_1 = a_3 - \frac{a_2^2}{a_1}$$

$$b_2 = a_4 - \frac{a_2 a_3}{a_1}$$

$$b_3 = a_5 - \frac{a_3^2}{a_1}$$

If equation (A34) is integrated and the boundary condition (A37) is used,

$$\left(b_1\varphi_1''\right)' + \left(b_2\varphi_2''\right)' - 2(1-\mu)\left(a_1\varphi_1' + 2a_2\varphi_2'\right) = -\int_x^l p_2\,dx - \left(\frac{a_2}{a_1}\int_x^l\int_x^l p_1\,dx^2\right)' \qquad \text{(A41)}$$

Thus φ_1 and φ_2 are obtained by solving equations (A35) and (A41) with the boundary conditions (A36), (A38), (A39), and (A40). Subsequently, φ_0 can be obtained by solving equation (A33) with the boundary conditions $\varphi_0(0) = \varphi_0'(0) = 0$.

Stresses.- After the approximate deflection of the plate is determined from equations (A18) and (A22) or from equations (A33), (A35), and (A41), the extreme-fiber stresses may be calculated from the well-known equations of thin-plate theory, which are (see, for example, reference 9):

$$\sigma_x = \frac{6D}{t^2}\left(\frac{\partial^2 w}{\partial x^2} + \mu \frac{\partial^2 w}{\partial y^2}\right)$$

$$\sigma_y = \frac{6D}{t^2}\left(\frac{\partial^2 w}{\partial y^2} + \mu \frac{\partial^2 w}{\partial x^2}\right)$$

$$\tau_{xy} = \frac{6(1 - \mu)D}{t^2} \frac{\partial^2 w}{\partial x \, \partial y}$$

The maximum principal stress σ at any point in the plate can be determined from

$$\sigma = \frac{\sigma_x + \sigma_y}{2} \pm \frac{1}{2}\sqrt{(\sigma_x - \sigma_y)^2 + 4\tau_{xy}^2}$$

APPENDIX B

EXACT SOLUTIONS OF DIFFERENTIAL EQUATIONS FOR SOME SPECIFIC DELTA-PLATE PROBLEMS

The differential equations of appendix A for linear and parabolic chordwise deflections are solved exactly for uniformly loaded delta plates of constant thickness and of diamond chordwise cross section with constant thickness ratio. The equations for deflections obtained by the linear theory are presented in terms of the aspect-ratio parameter λ for both kinds of delta plates. The equations for deflections obtained by the parabolic theory are presented for $\frac{l}{c} = 1$ and $\frac{\sqrt{3}}{3}$ with $\mu = \frac{1}{3}$ for the constant-thickness delta plate and for $\frac{l}{c} = 1$, also with $\mu = \frac{1}{3}$, for the delta plate of diamond chordwise cross section with constant thickness ratio.

If the x-axis is passed through the edge perpendicular to the root and the substitution $x_1 = 1 - \frac{x}{l}$ is made, the differential equations are clearly of the homogeneous type for which the solutions are of the form x_1^{γ} where γ is a constant. For the configurations considered, the functions that define the plan form (see fig. 1) are then $c_1(x) = 0$ and $c_2(x) = cx_1$, where c is the root chord. In all the equations of this appendix the primes denote differentiation with respect to the new independent variable x_1.

Delta Plate of Uniform Thickness under Uniform Load

Since the stiffness D is a constant for uniform-thickness plates, the coefficients in the differential equations (see equation (A4)) become

$$a_n = \frac{Dc^n}{n} x_1^n \tag{B1a}$$

$$b_1 = a_3 - \frac{a_2^2}{a_1} = \frac{Dc^3}{12} x_1^3 \tag{B1b}$$

$$b_2 = a_4 - \frac{a_2 a_3}{a_1} = \frac{Dc^4}{12} x_1^4 \tag{B1c}$$

$$b_3 = a_5 - \frac{a_3^2}{a_1} = \frac{4Dc^5}{45} x_1^5 \tag{B1d}$$

$$p_n = \frac{pc^n}{n} x_1^n \tag{B1e}$$

Solution for linear chordwise deflections.- If the coefficients given by equations (B1) are substituted into equations (A22) and (A18) and the independent variable is changed to $x_1 = 1 - \frac{x}{l}$, the following equations for linear chordwise deflections result:

$$\left(x_1^3 \varphi_1''\right)' - 16\lambda^2 x_1 \varphi_1' = -2 \frac{pl^4}{Dc} x_1^3 \tag{B2}$$

$$\varphi_0'' = -\frac{c}{2} x_1 \varphi_1'' + \frac{pl^4}{6D} x_1^2 \tag{B3}$$

where

$$\lambda = \frac{l}{c}\sqrt{\frac{3}{2}(1 - \mu)}$$

The boundary conditions to be used with these equations are obtained from equations (A13) and (A20) and are

$$\varphi_0(1) = \varphi_0'(1) = \varphi_1(1) = \varphi_1'(1) = 0 \tag{B4}$$

$$\left(x_1^3 \varphi_1''\right)_{x_1=0} = 0 \tag{B5}$$

The general solution of equation (B2) is

$$\varphi_1' = A_1 x_1^{\gamma-1} + A_2 x_1^{-\gamma-1} - \frac{x_1^2}{4(1 - 2\lambda^2)} \frac{pl^4}{Dc} \tag{B6}$$

where

$$\gamma = \sqrt{1 + 16\lambda^2}$$

and A_1 and A_2 are arbitrary constants. Since λ^2 is inherently positive, the boundary condition (B5) requires that $A_2 = 0$. One integration of equation (B6) and the application of the conditions $\varphi_1(1) = \varphi_1'(1) = 0$ yields

$$\varphi_1 = \frac{1}{4(1 - 2\lambda^2)} \frac{pl^4}{Dc} \left(\frac{x_1^{\gamma} - 1}{\gamma} - \frac{x_1^3 - 1}{3} \right) \tag{B7}$$

If equation (B3) is solved for φ_0 with the conditions $\varphi_0(1) = \varphi_0'(1) = 0$, the result is

$$\varphi_0 = \frac{pl^4}{8D} \frac{1}{1 - 2\lambda^2} \left[\frac{2}{9}(5 - 4\lambda^2) \left(1 - x_1 - \frac{1 - x_1^4}{4} \right) - \frac{\gamma - 1}{\gamma} \left(1 - x_1 - \frac{1 - x_1^{\gamma+1}}{\gamma + 1} \right) \right] \tag{B8}$$

Substitution of equations (B7) and (B8) into the equation

$$w = \varphi_0 + y\varphi_1$$

gives the expression for the deflection w of the plate under the assumption of linear chordwise deflections.

Solution for parabolic chordwise deflections.- If the coefficients given by equations (B1) are substituted into equations (A41), (A35),

and (A33) and the independent variable is again changed to $x_1 = 1 - \frac{x}{l}$, the following equations for parabolic chordwise deflections result:

$$\left(x_1^3\varphi_1''\right)' + \left(x_1^4 c\varphi_2''\right)' - 16\lambda^2\left(x_1\varphi_1' + x_1^2 c\varphi_2'\right) = -2\frac{pl^4}{Dc}x_1^3 \tag{B9}$$

$$\left(x_1^4\varphi_1''\right)'' + \frac{16}{15}\left(x_1^5 c\varphi_2''\right)'' - 16\lambda^2\left[\left(x_1^2\varphi_1'\right)' + \frac{4}{3}\left(x_1^3 c\varphi_2'\right)'\right] + \frac{64}{3}\lambda^4\frac{1+\mu}{1-\mu}x_1 c\varphi_2 = -\frac{4}{3}\left(7 + \frac{2\mu\lambda^2}{1-\mu}\right)\frac{pl^4}{Dc}x_1^3 \tag{B10}$$

$$\varphi_0'' = -\frac{c}{2}x_1\varphi_1'' - \frac{c^2}{3}x_1^2\varphi_2'' - 2\mu l^2\varphi_2 + \frac{pl^4}{D}\frac{x_1^2}{6} \tag{B11}$$

The boundary conditions to be used with these equations are

$$\varphi_0(1) = \varphi_0'(1) = \varphi_1(1) = \varphi_1'(1) = \varphi_2(1) = \varphi_2'(1) = 0 \tag{B12}$$

$$\left(x_1^3\varphi_1'' + x_1^4 c\varphi_2''\right)_{x_1=0} = 0 \tag{B13}$$

$$\left(x_1^4\varphi_1'' + \frac{16}{15}x_1^5 c\varphi_2''\right)_{x_1=0} = 0 \tag{B14}$$

$$\left[\left(x_1^4\varphi_1''\right)' + \frac{16}{15}\left(x_1^5 c\varphi_2''\right)' - 16\lambda^2\left(x_1^2\varphi_1' + \frac{4}{3}x_1^3 c\varphi_2'\right)\right]_{x_1=0} = 0 \tag{B15}$$

The homogeneous solutions of the simultaneous equations (B9) and (B10) are of the form

$$\varphi_1' = Ax_1^{\gamma-1}$$

$$\varphi_2 = Bx_1^{\gamma-1}$$

Substitution of these expressions into the homogeneous parts of equations (B9) and (B10) leads to the following characteristic equation from which γ may be determined:

$$\gamma^6 - 6(1 + 16\lambda^2)\gamma^4 + \left[320\left(4 + \frac{1 + \mu}{1 - \mu}\right)\lambda^4 + 480\lambda^2 + 9\right]\gamma^2 -$$

$$4\left[1280\,\frac{1 + \mu}{1 - \mu}\,\lambda^6 + 80\left(4 + \frac{1 + \mu}{1 - \mu}\right)\lambda^4 + 96\lambda^2 + 1\right] = 0 \qquad \text{(B16)}$$

and gives the following relationship between A and B:

$$A = -(\gamma - 1)\left[\frac{(\gamma - 2)(\gamma + 1) - 16\lambda^2}{\gamma^2 - 1 - 16\lambda^2}\right]cB$$

The particular solutions for uniform loading are given by

$$\varphi_1' = A_p x_1^2$$

$$\varphi_2 = B_p x_1^2$$

where

$$A_p = \frac{1}{2}\,\frac{4\,\frac{3\mu + 1}{1 - \mu}\,\lambda^4 - 2\,\frac{2 - \mu}{1 - \mu}\,\lambda^2 + 1}{8\,\frac{1 + \mu}{1 - \mu}(2\lambda^2 - 1)\lambda^4 - (8\lambda^2 - 1)(4\lambda^2 - 1)}\,\frac{pl^4}{Dc}$$

$$B_p = -\frac{1}{4}\,\frac{\frac{4\mu\lambda^2}{1 - \mu}(2\lambda^2 - 1) + 1 + 4\lambda^2}{8\,\frac{1 + \mu}{1 - \mu}(2\lambda^2 - 1)\lambda^4 - (8\lambda^2 - 1)(4\lambda^2 - 1)}\,\frac{pl^4}{Dc^2}$$

The general solution is the sum of the homogeneous solutions and the particular integral

$$\varphi_1' = \sum_{n=1}^{6} A_n x_1^{\gamma_n - 1} + A_p x_1^2$$

$$\varphi_2 = \sum_{n=1}^{6} B_n x_1^{\gamma_n - 1} + B_p x_1^2 \qquad \text{(B17)}$$

where the values γ_n are the six roots of the characteristic equation (B16) and the coefficients A_n and B_n are the coefficients corresponding to each of these roots. After integration φ_1 becomes

$$\varphi_1 = \sum_{n=1}^{6} A_n \frac{x_1^{\gamma_n}}{\gamma_n} + A_p \frac{x_1^3}{3} + A_q \qquad \text{(B18)}$$

The general solution for φ_0 from equation (B11) is found to be

$$\varphi_0 = \sum_{n=1}^{6} C_n x_1^{\gamma_n + 1} + C_p x_1^4 + C_q x_1 + C_r \qquad \text{(B19)}$$

where, for $n = 1, 2, \ldots 6$,

$$C_n = -\frac{c}{\gamma_n(\gamma_n + 1)}\left\{\frac{\gamma_n - 1}{2} A_n + \frac{c}{3}\left[(\gamma_n - 1)(\gamma_n - 2) + \frac{4\mu\lambda^2}{1 - \mu}\right] B_n\right\}$$

and

$$C_p = -\frac{c}{12}\left[A_p + \frac{2c}{3}\left(1 + \frac{2\mu\lambda^2}{1 - \mu}\right) B_p - \frac{p l^4}{6Dc}\right]$$

The coefficients A_1 to A_6, A_q, C_q, and C_r must be determined by the boundary conditions (B12) to (B15).

A complete set of coefficients is given in the following table for delta plates with Poisson's ratio μ equal to 1/3 and with $\lambda = \frac{l}{c} = 1$ and $\frac{\sqrt{3}}{3}$. Deflection curves plotted from these results are shown in figures 2 and 3 in which the 45° plate corresponds to $\frac{l}{c} = 1$ and the 60° plate corresponds to $\frac{l}{c} = \frac{\sqrt{3}}{3}$.

m	γ_m		$A_m \frac{Dc}{pl^4}$		$B_m \frac{Dc^2}{pl^4}$		$C_m \frac{D}{pl^4}$	
	$\lambda = 1$	$\lambda = \frac{\sqrt{3}}{3}$	$\lambda = 1$	$\lambda = \frac{\sqrt{3}}{3}$	$\lambda = 1$	$\lambda = \frac{\sqrt{3}}{3}$	$\lambda = 1$	$\lambda = \frac{\sqrt{3}}{3}$
1	2.7034	1.5671	0.7378	0.09632	-0.3133	-0.1022	-0.02931	-0.003223
2	4.9437	3.6347	.02411	.3707	-.03039	-.4313	.003074	.01347
3	8.3816	4.7258	.03827	-.1766	-.006293	.07379	.000486	.002317
4	-2.7034	-1.5671	0	0	0	0	0	0
5	-4.9437	-3.6347	0	0	0	0	0	0
6	-8.3816	-4.7258	0	0	0	0	0	0
p	-------	-------	-.8000	-.2903	.3500	.4597	.04167	.004032
q	-------	-------	-.01557	-.02924	---------	--------	-.07152	-.08354
r	-------	-------	-------	-------	---------	--------	.05668	.06692

Substitution of equations (B17), (B18), and (B19) into the equation

$$w = \varphi_0 + y\varphi_1 + y^2\varphi_2$$

gives the expression for the deflection w of the plate under the assumption of parabolic chordwise deflection.

Delta Plate of Diamond Chordwise Cross Section with Constant Thickness Ratio under Uniform Load

For a delta plate of diamond chordwise cross section with a constant thickness ratio the thickness is a function of x and y and is given by the following equations:

$$t = 6t_{av}\frac{y}{c} \qquad \left(0 \leqq y \leqq \frac{cx_1}{2}\right)$$

$$t = 6t_{av}\left(x_1 - \frac{y}{c}\right) \qquad \left(\frac{cx_1}{2} \leqq y \leqq cx_1\right)$$

where t_{av} is the average thickness. From these expressions for the thickness the stiffness can be found and the coefficients in the differential equations become

$$\left.\begin{aligned}
a_1 &= \frac{27\bar{D}c}{4} x_1^4 \\
a_2 &= \frac{27\bar{D}c^2}{8} x_1^5 \\
a_3 &= \frac{9\bar{D}c^3}{5} x_1^6 \\
a_4 &= \frac{81\bar{D}c^4}{80} x_1^7 \\
a_5 &= \frac{2673\bar{D}c^5}{4480} x_1^8 \\
b_1 &= \frac{9\bar{D}c^3}{80} x_1^6 \\
b_2 &= \frac{9\bar{D}c^4}{80} x_1^7 \\
b_3 &= \frac{2613\bar{D}c^5}{22400} x_1^8 \\
p_n &= \frac{pc^n}{n} x_1^n
\end{aligned}\right\} \qquad \text{(B20)}$$

Solution for linear chordwise deflections.- By use of the coefficients given by equations (B20), equations (A22) and (A18) for linear chordwise deflections may be solved for φ_1 and φ_0. The steps in the solution are the same in form as those for the uniform-thickness plate and the resulting equations are:

$$\varphi_1 = \frac{40}{27\left(\gamma^2 - \frac{9}{4}\right)} \left(\frac{1 - x_1^{\gamma - \frac{3}{2}}}{\gamma - \frac{3}{2}} + \log_e x_1 \right) \frac{pl^4}{\bar{D}c} \qquad \text{(B21)}$$

and

$$\varphi_0 = \frac{1}{27}\left[\frac{20}{\gamma^2 - \frac{9}{4}}\frac{\gamma - \frac{5}{2}}{\gamma - \frac{3}{2}}\left(\frac{x_1^{\gamma - \frac{1}{2}} - 1}{\gamma - \frac{1}{2}} + 1 - x_1\right) + \left(\frac{20}{\gamma^2 - \frac{9}{4}} + \frac{2}{3}\right)\left(x_1 \log_e x_1 + 1 - x_1\right)\right]\frac{pl^4}{D} \tag{B22}$$

where

$$\gamma = \sqrt{\left(\frac{5}{2}\right)^2 + 80\lambda^2}$$

Solution for parabolic chordwise deflections.- By use of the coefficients given by equations (B20), equations (A41), (A35), and (A33) for parabolic chordwise deflections may be solved for φ_1, φ_2, and φ_0. The steps in the solution are again the same in form as those for the uniform-thickness plate and the resulting general expressions for φ_1, φ_2, and φ_0 are:

$$\varphi_1 = \sum_{n=1}^{6} A_n \frac{x_1^{\gamma_n - \frac{3}{2}} - 1}{\gamma_n - \frac{3}{2}} + A_p \log_e x_1 \tag{B23}$$

$$\varphi_2 = \sum_{n=1}^{6} B_n x_1^{\gamma_n - \frac{5}{2}} + B_p \frac{1}{x_1} \tag{B24}$$

$$\varphi_0 = \sum_{n=1}^{6} C_n x_1^{\gamma_n - \frac{1}{2}} + C_p x_1 \log_e x_1 + C_q x_1 + C_r \tag{B25}$$

where the exponents γ_n are the roots of the characteristic equation

$$\left(\gamma^2 - \frac{25}{4} - 80\lambda^2\right)\left[\frac{871}{840}\left(\gamma^2 - \frac{25}{4}\right)\left(\gamma^2 - \frac{49}{4}\right) - \frac{256}{3}\lambda^2\left(\gamma^2 - \frac{25}{4}\right) + \frac{320}{3}\frac{1+\mu}{1-\mu}\lambda^4\right] - \gamma^2\left(\gamma^2 - \frac{25}{4} - 80\lambda^2\right)^2 + \left[\frac{7}{2}\left(\gamma^2 - \frac{25}{4}\right) - 200\lambda^2\right]^2 = 0 \tag{B26}$$

For $n = 1, 2, \ldots 6$, A_n, B_n, and C_n are related by

$$B_n = -\frac{\gamma^2 - \frac{25}{4} - 80\lambda^2}{\left(\gamma - \frac{5}{2}\right)\left[\left(\gamma - \frac{7}{2}\right)\left(\gamma + \frac{5}{2}\right) - 80\lambda^2\right]}\frac{A_n}{c}$$

$$C_n = -\frac{c}{\gamma_n - \frac{3}{2}}\left\{\frac{\gamma_n - \frac{5}{2}}{2}A_n + \frac{4}{15}c\left[\left(\gamma_n - \frac{5}{2}\right)\left(\gamma_n - \frac{7}{2}\right) + \frac{5\mu\lambda^2}{1-\mu}\right]B_n\right\}$$

For uniform load the coefficients in the particular integrals of equations (B23), (B24), and (B25) are

$$A_p = \frac{10}{27}\frac{pl^4}{\bar{D}c}\frac{\frac{871}{7} + 1024\lambda^2 + 320\frac{1+\mu}{1-\mu}\lambda^4 - 16\left(5 + \frac{2\mu}{1-\mu}\lambda^2\right)\left(10\lambda^2 + 1\right)}{\left(20\lambda^2 + 1\right)\left(\frac{871}{7} + 1024\lambda^2 + 320\frac{1+\mu}{1-\mu}\lambda^4\right) - 120\left(16\lambda^2 + 1\right)\left(10\lambda^2 + 1\right)}$$

$$B_p = \frac{40}{27}\frac{pl^4}{\bar{D}c^2}\frac{15\left(16\lambda^2 + 1\right) - 2\left(20\lambda^2 + 1\right)\left(5 + \frac{2\mu\lambda^2}{1-\mu}\right)}{\left(20\lambda^2 + 1\right)\left(\frac{871}{7} + 1024\lambda^2 + 320\frac{1+\mu}{1-\mu}\lambda^4\right) - 120\left(16\lambda^2 + 1\right)\left(10\lambda^2 + 1\right)}$$

$$C_p = \frac{c}{2} A_p - \frac{8}{15} c^2\left(1 + \frac{5}{2}\frac{\mu\lambda^2}{1-\mu}\right)B_p + \frac{2}{81}\frac{pl^4}{\bar{D}}$$

The coefficients A_1 to A_6, A_q, C_q, and C_r are again determined by the boundary conditions (A26), (A36), (A38), and (A39) in which the coefficients given by equations (B20) are substituted.

For Poisson's ratio μ equal to 1/3 and $\lambda = \frac{l}{c} = 1$, the solution of the characteristic equation (B26) leads to two real values and two pairs of complex conjugate values for γ. The identity

$$x_1^{a\pm ib} \equiv x_1^a \cos\left(b \log_e x_1\right) \pm i x_1^a \sin\left(b \log_e x_1\right)$$

was therefore used to transform the terms involving the complex conjugate values into real form. If $\frac{l}{c} = 1$ and $\mu = \frac{1}{3}$, the solution is

$$\varphi_2 = \frac{pl^4}{\bar{D}c^2}\left[0.004070x_1^{3.947} - 0.004363x_1^{8.075}\cos\left(2.825 \log_e x_1\right) + 0.006893x_1^{8.075}\sin\left(2.825 \log_e x_1\right) + 0.000294\frac{1}{x_1}\right]$$

$$\varphi_1 = \frac{pl^4}{\bar{D}c}\left[-0.003896x_1^{4.947} + 0.002134x_1^{9.075}\cos\left(2.825 \log_e x_1\right) - 0.006381x_1^{9.075}\sin\left(2.825 \log_e x_1\right) + 0.01794 \log_e x_1 + 0.001763\right]$$

$$\varphi_0 = \frac{pl^4}{\bar{D}}\left[0.0007715x_1^{5.947} - 0.0000708x_1^{10.075}\cos\left(2.825 \log_e x_1\right) + 0.001234x_1^{10.075}\sin\left(2.825 \log_e x_1\right) + 0.03331x_1 \log_e x_1 - 0.04096x_1 + 0.04026\right]$$

APPENDIX C

NUMERICAL PROCEDURE FOR SOLVING DIFFERENTIAL EQUATIONS

In cases where the equations of the present theory cannot be solved exactly, a numerical method must be used. In this appendix, equations (A19) and equations (A34) and (A35) are set up in difference form for numerical solution. Initially the assumption is made that the functions involved in the differential equations are continuous and non-singular. In this case, first and second derivatives can be expressed by the standard difference forms

$$\left(\frac{d^2y}{dx^2}\right)_n = \frac{y_{n+1} - 2y_n + y_{n-1}}{\epsilon^2}$$

$$\left(\frac{dy}{dx}\right)_n = \frac{y_{n+\frac{1}{2}} - y_{n-\frac{1}{2}}}{\epsilon}$$

where ϵ is the distance between equally spaced station points.

In the following development five equally spaced spanwise stations are used; however, the extension to a different number of stations can be readily made.

First, consider equation (A19) resulting from the linear theory

$$\left(b_1\varphi_1''\right)'' - 2(1 - \mu)\left(a_1\varphi_1'\right)' = p_2 - \left(\frac{a_2}{a_1}\int_x^l \int_x^l p_1(x)\, dx^2\right)'' = q_1$$

Because of the nature of the tip boundary conditions for this equation, it can be conveniently put in the form

$$T' = q_1 \tag{C1}$$

where

$$T = \left(b_1\varphi_1''\right)' - 2(1 - \mu)a_1\varphi_1'$$

In finding the difference equation equivalent to equation (C1), the quantity $\left(b_1\varphi_1''\right)'$ is found in matrix form; from this expression is subtracted the matrix equivalent of $2(1 - \mu)a_1\varphi_1'$; the resulting expression for T is multiplied by a differentiating matrix; and the product is equated to the right-hand side.

The quantity $\left(b_1\varphi_1''\right)'$ at the half-stations can be expressed in matrix form as follows:

$$\begin{vmatrix} \varphi_1''_0 \\ \varphi_1''_1 \\ \varphi_1''_2 \\ \varphi_1''_3 \\ \varphi_1''_4 \end{vmatrix} = \frac{1}{\epsilon^2} \begin{bmatrix} 1 & -2 & 1 & & & & \\ & 1 & -2 & 1 & & & \\ & & 1 & -2 & 1 & & \\ & & & 1 & -2 & 1 & \\ & & & & 1 & -2 & 1 \end{bmatrix} \begin{vmatrix} \varphi_{1-1} \\ \varphi_{10} \\ \varphi_{11} \\ \varphi_{12} \\ \varphi_{13} \\ \varphi_{14} \\ \varphi_{15} \end{vmatrix} \qquad \text{(C2)}$$

where the second subscript denotes the station point, the subscript at the root station being 0 and at the tip 5. The root boundary conditions are now applied; namely,

$$\varphi_1(0) = 0 = \varphi_{10}$$

$$\varphi_1'(0) = 0 = \frac{\varphi_{11} - \varphi_{1-1}}{2\epsilon}$$

Thus, after the values of $\varphi_{10} = 0$ and $\varphi_{1-1} = \varphi_{11}$ are substituted, equation (C2) becomes

$$\begin{vmatrix} \varphi_1''_0 \\ \varphi_1''_1 \\ \varphi_1''_2 \\ \varphi_1''_3 \\ \varphi_1''_4 \end{vmatrix} = \frac{1}{\epsilon^2} \begin{bmatrix} 2 & & & & \\ -2 & 1 & & & \\ 1 & -2 & 1 & & \\ & 1 & -2 & 1 & \\ & & 1 & -2 & 1 \end{bmatrix} \begin{vmatrix} \varphi_{11} \\ \varphi_{12} \\ \varphi_{13} \\ \varphi_{14} \\ \varphi_{15} \end{vmatrix}$$

Therefore,

$$\begin{vmatrix} (b_1\varphi_1'')_0 \\ (b_1\varphi_1'')_1 \\ (b_1\varphi_1'')_2 \\ (b_1\varphi_1'')_3 \\ (b_1\varphi_1'')_4 \end{vmatrix} = \frac{1}{\epsilon^2} \begin{bmatrix} b_{10} & & & & \\ & b_{11} & & & \\ & & b_{12} & & \\ & & & b_{13} & \\ & & & & b_{14} \end{bmatrix} \begin{bmatrix} 2 & & & & \\ -2 & 1 & & & \\ 1 & -2 & 1 & & \\ & 1 & -2 & 1 & \\ & & 1 & -2 & 1 \end{bmatrix} \begin{vmatrix} \varphi_{11} \\ \varphi_{12} \\ \varphi_{13} \\ \varphi_{14} \\ \varphi_{15} \end{vmatrix} \qquad (C3)$$

One of the tip boundary conditions is

$$(b_1\varphi_1'')_{x=l} = 0 = (b_1\varphi_1'')_5$$

Thus,

$$\begin{vmatrix} (b_1\varphi_1'')'_{1/2} \\ (b_1\varphi_1'')'_{3/2} \\ (b_1\varphi_1'')'_{5/2} \\ (b_1\varphi_1'')'_{7/2} \\ (b_1\varphi_1'')'_{9/2} \end{vmatrix} = \frac{1}{\epsilon} \begin{bmatrix} -1 & 1 & & & \\ & -1 & 1 & & \\ & & -1 & 1 & \\ & & & -1 & 1 \\ & & & & -1 \end{bmatrix} \begin{vmatrix} (b_1\varphi_1'')_0 \\ (b_1\varphi_1'')_1 \\ (b_1\varphi_1'')_2 \\ (b_1\varphi_1'')_3 \\ (b_1\varphi_1'')_4 \end{vmatrix} \qquad (C4)$$

The matrix equivalent for the second term of T is

$$2(1-\mu)\begin{vmatrix}(a_1\varphi_1')_{1/2}\\(a_1\varphi_1')_{3/2}\\(a_1\varphi_1')_{5/2}\\(a_1\varphi_1')_{7/2}\\(a_1\varphi_1')_{9/2}\end{vmatrix} = \frac{2(1-\mu)}{\epsilon}\begin{bmatrix}a_{1,1/2}&&&&\\&a_{1,3/2}&&&\\&&a_{1,5/2}&&\\&&&a_{1,7/2}&\\&&&&a_{1,9/2}\end{bmatrix}\begin{bmatrix}1&&&&\\-1&1&&&\\&-1&1&&\\&&-1&1&\\&&&-1&1\end{bmatrix}\begin{vmatrix}\varphi_{11}\\\varphi_{12}\\\varphi_{13}\\\varphi_{14}\\\varphi_{15}\end{vmatrix}$$

Therefore T becomes

$$\begin{vmatrix}T_{1/2}\\T_{3/2}\\T_{5/2}\\T_{7/2}\\T_{9/2}\end{vmatrix} = \left\{\frac{1}{\epsilon^3}\begin{bmatrix}-1&1&&&\\&-1&1&&\\&&-1&1&\\&&&-1&1\\&&&&-1\end{bmatrix}\begin{bmatrix}b_{10}&&&&\\&b_{11}&&&\\&&b_{12}&&\\&&&b_{13}&\\&&&&b_{14}\end{bmatrix}\begin{bmatrix}2&&&&\\-2&1&&&\\1&-2&1&&\\&1&-2&1&\\&&1&-2&1\end{bmatrix} - \right.$$

$$\left.\frac{2(1-\mu)}{\epsilon}\begin{bmatrix}a_{1,1/2}&&&&\\&a_{1,3/2}&&&\\&&a_{1,5/2}&&\\&&&a_{1,7/2}&\\&&&&a_{1,9/2}\end{bmatrix}\begin{bmatrix}1&&&&\\-1&1&&&\\&-1&1&&\\&&-1&1&\\&&&-1&1\end{bmatrix}\right\}\begin{vmatrix}\varphi_{11}\\\varphi_{12}\\\varphi_{13}\\\varphi_{14}\\\varphi_{15}\end{vmatrix} \qquad (C5)$$

The right-hand side of equation (C1) can now be equated to the derivative of equation (C5); thus,

$$\begin{vmatrix} q_{11} \\ q_{12} \\ q_{13} \\ q_{14} \end{vmatrix} = \frac{1}{\epsilon} \begin{bmatrix} -1 & 1 & & & \\ & -1 & 1 & & \\ & & -1 & 1 & \\ & & & -1 & 1 \end{bmatrix} \begin{vmatrix} T_{1/2} \\ T_{3/2} \\ T_{5/2} \\ T_{7/2} \\ T_{9/2} \end{vmatrix}$$

In order to obtain q_{15}, the boundary condition

$$T = 0$$

at $x = l$ must be used. In other words, T goes from $T_{9/2}$ at station $4\frac{1}{2}$ to 0 at station 5. A straight line drawn between these two points would have the slope $-\frac{2T_{9/2}}{\epsilon}$. The value of q_{15} is considered to be this slope; therefore,

$$\begin{vmatrix} q_{11} \\ q_{12} \\ q_{13} \\ q_{14} \\ q_{15}/2 \end{vmatrix} = \frac{1}{\epsilon} \begin{bmatrix} -1 & 1 & & & \\ & -1 & 1 & & \\ & & -1 & 1 & \\ & & & -1 & 1 \\ & & & & -1 \end{bmatrix} \begin{vmatrix} T_{1/2} \\ T_{3/2} \\ T_{5/2} \\ T_{7/2} \\ T_{9/2} \end{vmatrix}$$

or

$$\begin{vmatrix} q_{11} \\ q_{12} \\ q_{13} \\ q_{14} \\ q_{15}/2 \end{vmatrix} = \left\{ \frac{1}{\epsilon^4} \begin{bmatrix} 1 & -2 & 1 & & \\ & 1 & -2 & 1 & \\ & & 1 & -2 & 1 \\ & & & 1 & -2 \\ & & & & 1 \end{bmatrix} \begin{bmatrix} b_{10} & & & & \\ & b_{11} & & & \\ & & b_{12} & & \\ & & & b_{13} & \\ & & & & b_{14} \end{bmatrix} \begin{bmatrix} 2 & & & & \\ -2 & 1 & & & \\ 1 & -2 & 1 & & \\ & 1 & -2 & 1 & \\ & & 1 & -2 & 1 \end{bmatrix} - \right.$$

$$\left. \frac{2(1-\mu)}{\epsilon^2} \begin{bmatrix} -1 & 1 & & & \\ & -1 & 1 & & \\ & & -1 & 1 & \\ & & & -1 & 1 \\ & & & & -1 \end{bmatrix} \begin{bmatrix} a_{1,1/2} & & & & \\ & a_{1,3/2} & & & \\ & & a_{1,5/2} & & \\ & & & a_{1,7/2} & \\ & & & & a_{1,9/2} \end{bmatrix} \begin{bmatrix} 1 & & & & \\ -1 & 1 & & & \\ & -1 & 1 & & \\ & & -1 & 1 & \\ & & & -1 & 1 \end{bmatrix} \right\} \begin{vmatrix} \varphi_{11} \\ \varphi_{12} \\ \varphi_{13} \\ \varphi_{14} \\ \varphi_{15} \end{vmatrix}$$

If the matrix multiplication is carried out, the difference equivalent of equation (C1) finally becomes

$$\begin{vmatrix} q_{11} \\ q_{12} \\ q_{13} \\ q_{14} \\ q_{15}/2 \end{vmatrix} = \left\{ \frac{1}{\epsilon^4} \begin{bmatrix} C_1 \end{bmatrix} - \frac{2(1-\mu)}{\epsilon^2} \begin{bmatrix} D_1 \end{bmatrix} \right\} \begin{vmatrix} \varphi_{11} \\ \varphi_{12} \\ \varphi_{13} \\ \varphi_{14} \\ \varphi_{15} \end{vmatrix} \tag{C6}$$

where

$$[C_1] = \begin{bmatrix} 2b_{10} + 4b_{11} + b_{12} & -2b_{11} - 2b_{12} & b_{12} & & \\ -2b_{11} - 2b_{12} & b_{11} + 4b_{12} + b_{13} & -2b_{12} - 2b_{13} & b_{13} & \\ b_{12} & -2b_{12} - 2b_{13} & b_{12} + 4b_{13} + b_{14} & -2b_{13} - 2b_{14} & b_{14} \\ & b_{13} & -2b_{13} - 2b_{14} & b_{13} + 4b_{14} & -2b_{14} \\ & & b_{14} & -2b_{14} & b_{14} \end{bmatrix}$$

$$[D_1] = \begin{bmatrix} -a_{1,1/2} - a_{1,3/2} & a_{1,3/2} & & & \\ a_{1,3/2} & -a_{1,3/2} - a_{1,5/2} & a_{1,5/2} & & \\ & a_{1,5/2} & -a_{1,5/2} - a_{1,7/2} & a_{1,7/2} & \\ & & a_{1,7/2} & -a_{1,7/2} - a_{1,9/2} & a_{1,9/2} \\ & & & a_{1,9/2} & -a_{1,9/2} \end{bmatrix}$$

In order to determine φ_0 from φ_1, use must be made of equation (A18)

$$\varphi_0'' = \frac{1}{a_1} \int_x^l \int_x^l p_1 \, dx^2 - \frac{a_2}{a_1} \varphi_1''$$

or, by use of the boundary condition $\varphi_0(0) = \varphi_0'(0) = 0$,

$$\varphi_0 = \int_0^x \int_0^x \frac{1}{a_1} \int_x^l \int_x^l p_1 \, dx^4 - \int_0^x \int_0^x \frac{a_2}{a_1} \varphi_1'' \, dx^2 \qquad (C7)$$

In matrix form equation (C7) becomes

$$\begin{vmatrix}\varphi_{01}\\ \varphi_{02}\\ \varphi_{03}\\ \varphi_{04}\\ \varphi_{05}\end{vmatrix} = \epsilon^4 \begin{bmatrix}1 & & & & \\ 1 & 1 & & & \\ 1 & 1 & 1 & & \\ 1 & 1 & 1 & 1 & \\ 1 & 1 & 1 & 1 & 1\end{bmatrix}\begin{bmatrix}1/2 & & & & \\ 1/2 & 1 & & & \\ 1/2 & 1 & 1 & & \\ 1/2 & 1 & 1 & 1 & \\ 1/2 & 1 & 1 & 1 & 1\end{bmatrix}\begin{bmatrix}1/a_{10} & & & & \\ & 1/a_{11} & & & \\ & & 1/a_{12} & & \\ & & & 1/a_{13} & \\ & & & & 1/a_{14}\end{bmatrix}\begin{bmatrix}1 & 1 & 1 & 1 & 1\\ & 1 & 1 & 1 & 1\\ & & 1 & 1 & 1\\ & & & 1 & 1\\ & & & & 1\end{bmatrix}\begin{bmatrix}1 & 1 & 1 & 1 & 1\\ & 1 & 1 & 1 & 1\\ & & 1 & 1 & 1\\ & & & 1 & 1\\ & & & & 1\end{bmatrix}\begin{vmatrix}p_{11}\\ p_{12}\\ p_{13}\\ p_{14}\\ p_{15}/2\end{vmatrix} -$$

$$\begin{bmatrix}1 & & & & \\ 1 & 1 & & & \\ 1 & 1 & 1 & & \\ 1 & 1 & 1 & 1 & \\ 1 & 1 & 1 & 1 & 1\end{bmatrix}\begin{bmatrix}1/2 & & & & \\ 1/2 & 1 & & & \\ 1/2 & 1 & 1 & & \\ 1/2 & 1 & 1 & 1 & \\ 1/2 & 1 & 1 & 1 & 1\end{bmatrix}\begin{bmatrix}(a_2/a_1)_0 & & & & \\ & (a_2/a_1)_1 & & & \\ & & (a_2/a_1)_2 & & \\ & & & (a_2/a_1)_3 & \\ & & & & (a_2/a_1)_4\end{bmatrix}\begin{bmatrix}2 & & & & \\ -2 & 1 & & & \\ 1 & -2 & 1 & & \\ & 1 & -2 & 1 & \\ & & 1 & -2 & 1\end{bmatrix}\begin{vmatrix}\varphi_{11}\\ \varphi_{12}\\ \varphi_{13}\\ \varphi_{14}\\ \varphi_{15}\end{vmatrix} \quad (C8)$$

Thus, if the values of q_1 (which can be determined numerically or analytically according to preference and feasibility) are known, the values of φ_1 can be found by solving equation (C6) and the values of φ_0 in turn by means of equation (C8).

The foregoing development applies to the case where only linear chordwise deformations are allowed. A similar procedure is followed in expressing the differential equations pertaining to the parabolic theory in difference form; only the results are shown herein.

The matrix equivalent to equations (A34) and (A35) is

$$\begin{vmatrix} q_{11} \\ q_{12} \\ q_{13} \\ q_{14} \\ q_{15}/2 \\ q_{21} \\ q_{22} \\ q_{23} \\ q_{24} \\ q_{25}/2 \end{vmatrix} = \begin{bmatrix} & \\ \frac{1}{\epsilon^4}[C_1] - \frac{2(1-\mu)}{\epsilon^2}[D_1] & \frac{1}{\epsilon^4}[C_2] - \frac{4(1-\mu)}{\epsilon^2}[D_2] \\ & \\ & \\ \frac{1}{\epsilon^4}[C_2] - \frac{4(1-\mu)}{\epsilon^2}[D_2] & \frac{1}{\epsilon^4}[C_3] - \frac{8(1-\mu)}{\epsilon^2}[D_3] + 4(1-\mu^2)[E] \\ & \end{bmatrix} \begin{vmatrix} \varphi_{11} \\ \varphi_{12} \\ \varphi_{13} \\ \varphi_{14} \\ \varphi_{15} \\ \varphi_{21} \\ \varphi_{22} \\ \varphi_{23} \\ \varphi_{24} \\ \varphi_{25} \end{vmatrix} \tag{C9}$$

where

$$[C_n] = \begin{bmatrix} 2b_{n0} + 4b_{n1} + b_{n2} & -2b_{n1} - 2b_{n2} & b_{n2} & & \\ -2b_{n1} - 2b_{n2} & b_{n1} + 4b_{n2} + b_{n3} & -2b_{n2} - 2b_{n3} & b_{n3} & \\ b_{n2} & -2b_{n2} - 2b_{n3} & b_{n2} + 4b_{n3} + b_{n4} & -2b_{n3} - 2b_{n4} & b_{n4} \\ & b_{n3} & -2b_{n3} - 2b_{n4} & b_{n3} + 4b_{n4} & -2b_{n4} \\ & & b_{n4} & -2b_{n4} & b_{n4} \end{bmatrix}$$

$$[D_n] = \begin{bmatrix} -a_{n,1/2} - a_{n,3/2} & a_{n,3/2} & & & \\ a_{n,3/2} & -a_{n,3/2} - a_{n,5/2} & a_{n,5/2} & & \\ & a_{n,5/2} & -a_{n,5/2} - a_{n,7/2} & a_{n,7/2} & \\ & & a_{n,7/2} & -a_{n,7/2} - a_{n,9/2} & a_{n,9/2} \\ & & & a_{n,9/2} & -a_{n,9/2} \end{bmatrix}$$

$$[E] = \begin{bmatrix} a_{11} & & & & \\ & a_{12} & & & \\ & & a_{13} & & \\ & & & a_{14} & \\ & & & & a_{15} \end{bmatrix}$$

and q_1 and q_2 are the right-hand sides of equations (A34) and (A35), respectively; that is,

$$q_1 = p_2 - \left(\frac{a_2}{a_1}\int_x^l \int_x^l p_1 \, dx^2\right)''$$

$$q_2 = p_3 - 2\mu \int_x^l \int_x^l p_1 \, dx^2 - \left(\frac{a_3}{a_1}\int_x^l \int_x^l p_1 \, dx^2\right)''$$

With φ_1 and φ_2 known, φ_0 can be obtained by use of equation (A33)

$$\begin{bmatrix}\varphi_{01}\\ \varphi_{02}\\ \varphi_{03}\\ \varphi_{04}\\ \varphi_{05}\end{bmatrix} = \begin{bmatrix}1 & & & & \\ 1 & 1 & & & \\ 1 & 1 & 1 & & \\ 1 & 1 & 1 & 1 & \\ 1 & 1 & 1 & 1 & 1\end{bmatrix}\begin{bmatrix}1/2 & & & & \\ 1/2 & 1 & & & \\ 1/2 & 1 & 1 & & \\ 1/2 & 1 & 1 & 1 & \\ 1/2 & 1 & 1 & 1 & 1\end{bmatrix}\left\{\epsilon^4\begin{bmatrix}1/a_{10} & & & & \\ & 1/a_{11} & & & \\ & & 1/a_{12} & & \\ & & & 1/a_{13} & \\ & & & & 1/a_{14}\end{bmatrix}\begin{bmatrix}1 & 1 & 1 & 1 & 1\\ & 1 & 1 & 1 & 1\\ & & 1 & 1 & 1\\ & & & 1 & 1\\ & & & & 1\end{bmatrix}\begin{bmatrix}1 & 1 & 1 & 1 & 1\\ & 1 & 1 & 1 & 1\\ & & 1 & 1 & 1\\ & & & 1 & 1\\ & & & & 1\end{bmatrix}\begin{bmatrix}p_{11}\\ p_{12}\\ p_{13}\\ p_{14}\\ p_{15}/2\end{bmatrix} -$$

$$\begin{bmatrix}(a_2/a_1)_0 & & & & \\ & (a_2/a_1)_1 & & & \\ & & (a_2/a_1)_2 & & \\ & & & (a_2/a_1)_3 & \\ & & & & (a_2/a_1)_4\end{bmatrix}\begin{bmatrix}2 & & & & \\ -2 & 1 & & & \\ 1 & -2 & 1 & & \\ & 1 & -2 & 1 & \\ & & 1 & -2 & 1\end{bmatrix}\begin{bmatrix}\varphi_{11}\\ \varphi_{12}\\ \varphi_{13}\\ \varphi_{14}\\ \varphi_{15}\end{bmatrix} -$$

$$\begin{bmatrix}(a_3/a_1)_0 & & & & \\ & (a_3/a_1)_1 & & & \\ & & (a_3/a_1)_2 & & \\ & & & (a_3/a_1)_3 & \\ & & & & (a_3/a_1)_4\end{bmatrix}\begin{bmatrix}2 & & & & \\ -2 & 1 & & & \\ 1 & -2 & 1 & & \\ & 1 & -2 & 1 & \\ & & 1 & -2 & 1\end{bmatrix}\begin{bmatrix}\varphi_{21}\\ \varphi_{22}\\ \varphi_{23}\\ \varphi_{24}\\ \varphi_{25}\end{bmatrix} - 2\mu\epsilon^2\begin{bmatrix}\varphi_{21}\\ \varphi_{22}\\ \varphi_{23}\\ \varphi_{24}\\ \varphi_{25}\end{bmatrix}\Bigg\} \qquad \text{(C10)}$$

It should be noted that, as can be expected, the matrix equations (C6) and (C8) are merely special cases of equations (C9) and (C10), respectively. In addition, the square matrixes in equations (C6) and (C9) are symmetric, a result that is consistent with the fact that the differential equations under consideration are self-adjoint.

In the beginning of this appendix the assumption was made that the functions involved in the differential equations are continuous and nonsingular. The difference solution, however, may be adequate for some cases in which this assumption is not strictly correct. For instance, the deflections of a plate with a discontinuous stiffness distribution could conceivably be not very different from the deflections of a plate with a continuous stiffness distribution closely approximating the discontinuous distribution except in the neighborhood of the discontinuity. The results yielded by the difference solution in this case would be those associated with the continuous stiffness distribution. The number of stations may have to be increased, however, in order to minimize the inaccuracy introduced by the discontinuity or, in other cases, by a singularity. The case of the diamond-cross-section, constant-thickness-ratio delta plate, discussed in the body of this paper, is an example of a treatment of a singularity. In this case, although the solution is singular, adequate accuracy is obtained by the difference solution if ten equal intervals are used.

APPENDIX D

DEFLECTION AND STRESS EXPERIMENTS ON SOME TRIANGULAR CANTILEVER PLATES

Test specimens.- The specimens tested were: (1) a 45° right-triangular plate clamped along one leg and (2) a 60° right-triangular plate clamped along the longer leg. Each specimen, cut from 24S-T4 aluminum-alloy sheet of 0.250-inch thickness, had a length perpendicular to the clamped edge of 30 inches.

Method of testing.- Figure 12, a photograph of the test setup, shows the methods of clamping, loading, and measurement of deflections. A 1,000,000-pound clamping load (held constant during the test) was applied to the root area of each specimen and a uniform load of 0.204 psi was applied by 2-inch washers giving a tip deflection in each case of approximately 3/4 inch.

The deflections were measured by dial gages placed at the points indicated in figures 2 and 3.

Stresses were obtained from the 45° specimen only. On this specimen, 13 resistance-wire rosette strain gages were placed at the points indicated in figure 5. The plate was loaded with 2-inch washers in four increments of 0.0847 psi per increment and the maximum tip deflection was 1.13 inches. Readings of all the strain gages were recorded at each increment of loading.

Analysis and discussion of data.- The deflection w was plotted in figures 2 and 3 in terms of the nondimensional parameter wD/pl^4, in which the elastic constants were taken as $E = 10.6 \times 10^6$ psi and $\mu = \frac{1}{3}$. It was found that the dial-gage forces reduced the tip deflection of the plate by approximately 2 percent; however, since this error is of the same order of magnitude as that in the material properties and from other sources, no corrections are made in the results presented.

The readings of each of the 39 individual strain gages were plotted against load, and the slope of each of the resulting linear curves was taken as the average strain per unit load of the individual gage. The principal stresses were then calculated and plotted in figure 5 in terms of the nondimensional parameter $\sigma t^2/pl^2$.

REFERENCES

1. Fung, Yuan-Cheng: Theoretical and Experimental Effect of Sweep upon Stress and Deflection Distribution in Aircraft Wings of High Solidity. Part 2. Stress and Deflection Analysis of Swept Plates. AF TR No. 5761, Part 2, Air Materiel Command, U.S. Air Force, Feb. 1950.

2. Williams, M. L.: Theoretical and Experimental Effect of Sweep upon the Stress and Deflection Distribution in Aircraft Wings of High Solidity. Part 6. The Plate Problem for a Cantilever Sector of Uniform Thickness. AF TR No. 5761, Part 6, Air Materiel Command, U.S. Air Force, Nov. 1950.

3. Shaw, F. S.: The Approximate Deflection of Thin Flat Triangular Cantilever Plates Subjected to Uniform Normal Load. Rep. SM. 154, Aero. Res. Lab. (Melbourne), June 1950.

4. Zahorski, A.: Mathematical Analysis of Cantilever Plates. Rep. No. GM-313, Northrop Aircraft, Inc., Jan. 1949.

5. Benson, Arthur S., and Niles, Alfred S.: Bending and Torsion of a Rhomboidal Cantilever Plate. Tech. Rep. No. 2, Air Forces Contract W33-038 Ac-16697, Guggenheim Aero. Lab., Stanford Univ., Oct. 15, 1948. (Also available as AF TR No. 5795, Part I, Air Materiel Command, U.S. Air Force, May 1950.)

6. Reissner, Eric, and Stein, Manuel: Torsion and Transverse Bending of Cantilever Plates. NACA TN 2369, 1951.

7. Schürch, H.: Zur Statik von dünnen Flugzeug-Tragflächen. Mitt. Nr. 2, Inst. für Flugzeugstatik und Flugzeugbau an der E.T.H., Leemann (Zürich), 1950.

8. Hrebec, G. M.: Theoretical and Experimental Effect of Sweep upon the Stress and Deflection Distribution in Aircraft Wings of High Solidity. Part 8. Some Experimental Data on the Deflection and Root Stresses in a Cantilever Triangular Plate of Constant Thickness with Varying Trailing Edge Sweep Angle. AF TR No. 5761, Part 8, Air Materiel Command, U.S. Air Force, Nov. 1950.

9. Timoshenko, S.: Theory of Elastic Stability. McGraw-Hill Book Co., Inc., 1936, ch. VI.

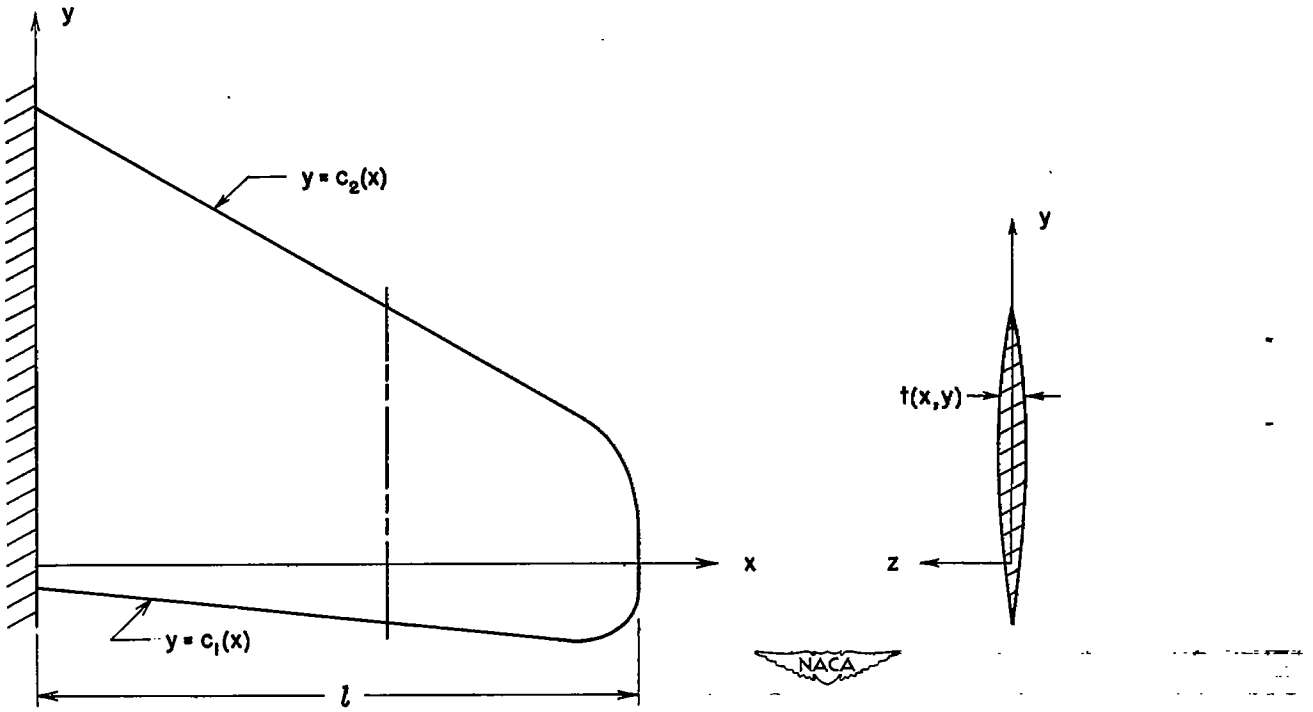

Figure 1.- Coordinate system used in the present analysis for a cantilever plate of arbitrary shape with arbitrary thickness variation.

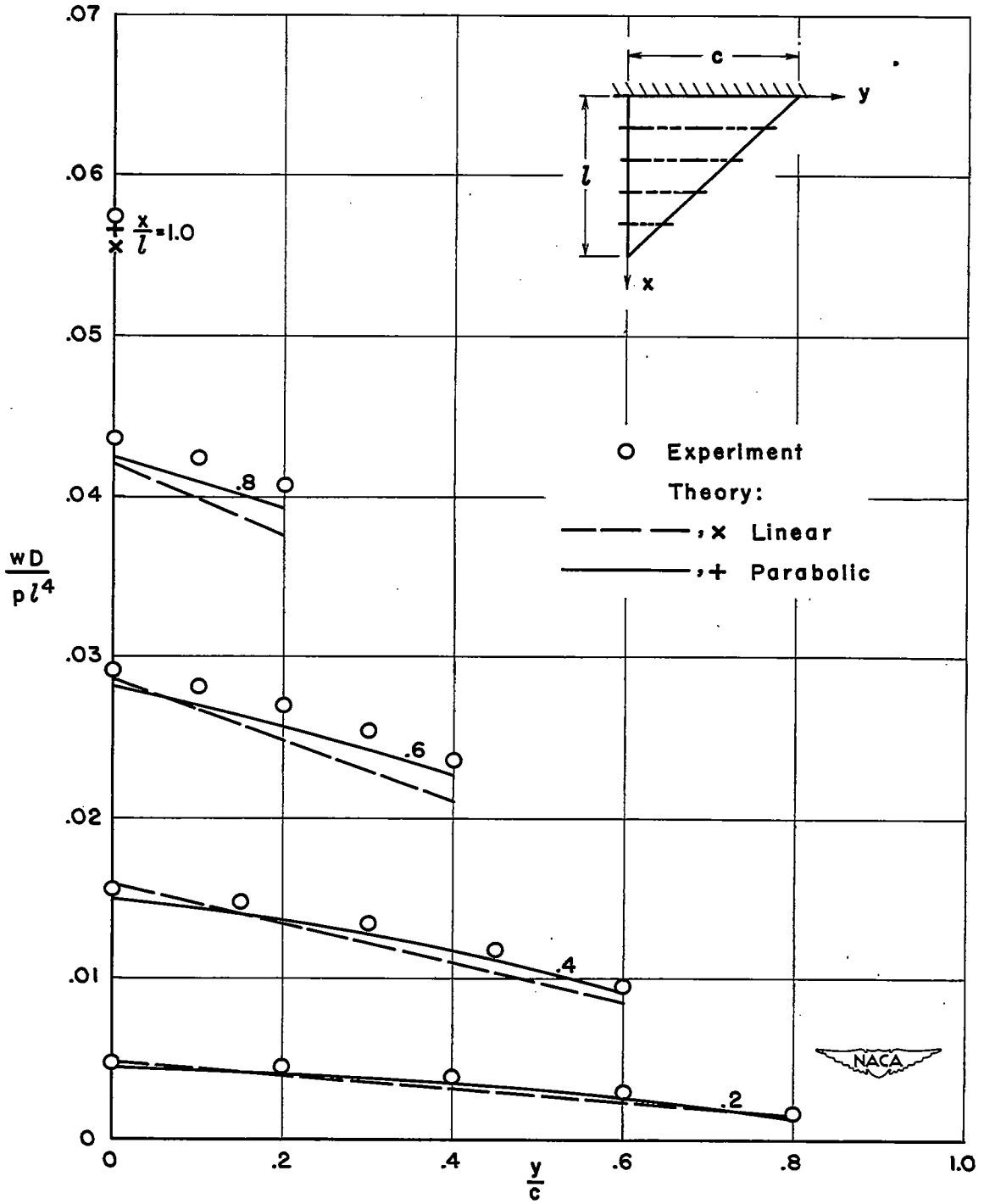

Figure 2.- Deflections of a 45° delta plate of uniform thickness under uniform load.

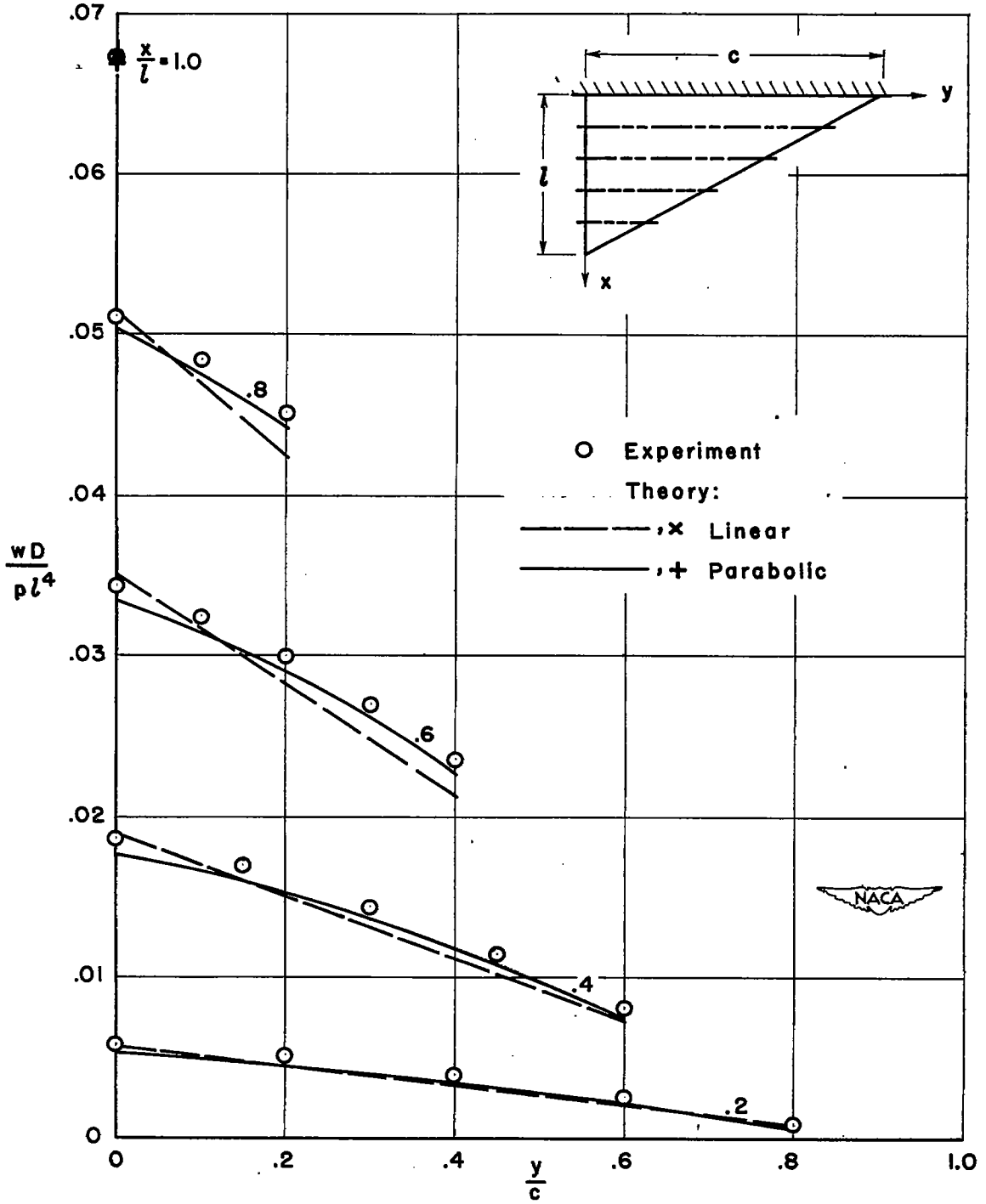

Figure 3.- Deflections of a 60° delta plate of uniform thickness under uniform load.

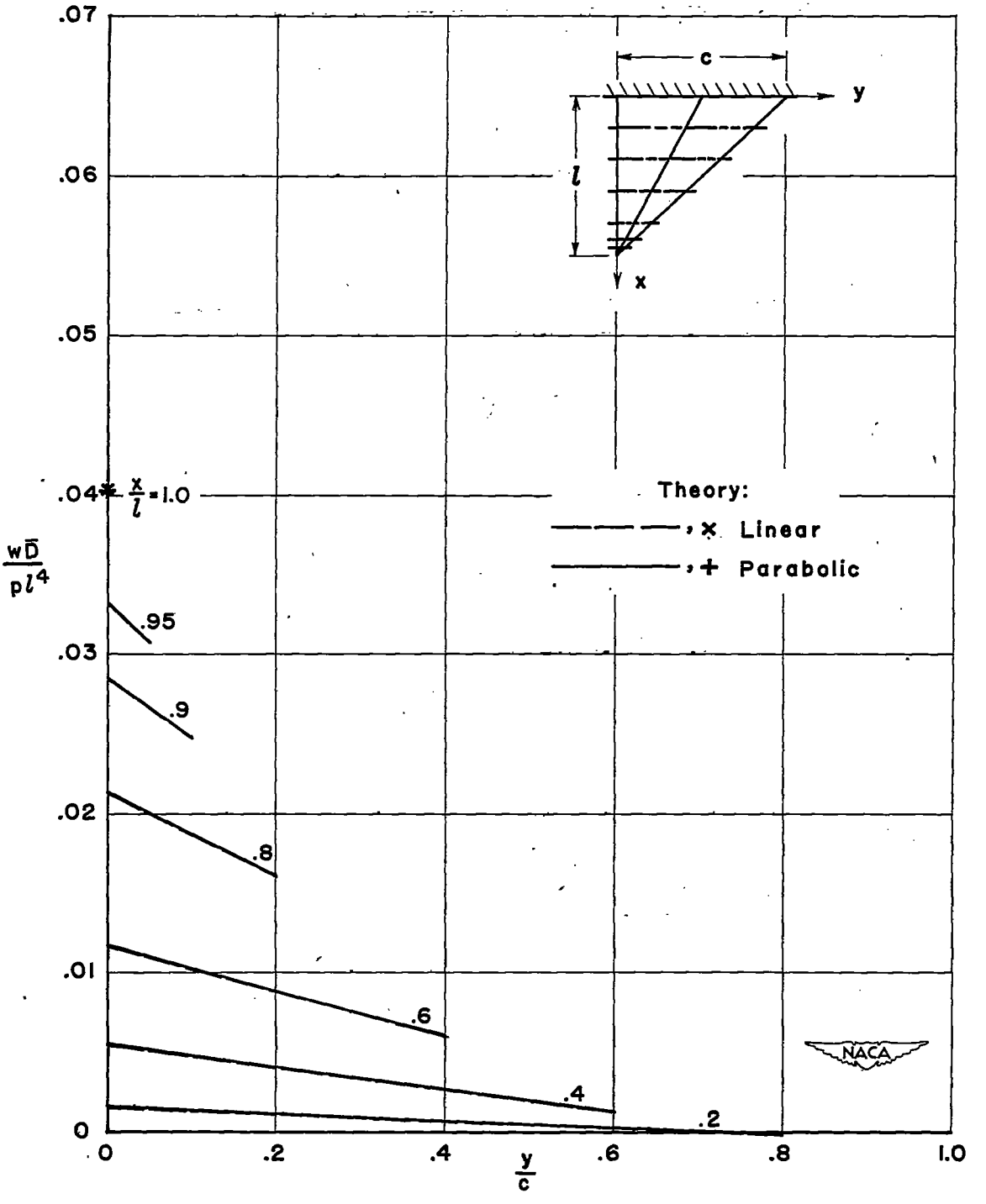

Figure 4.- Deflections of a 45° delta plate of diamond chordwise cross section and constant thickness ratio under uniform load.

$$\bar{D} = \frac{Et_{av}^3}{12(1 - \mu^2)}.$$

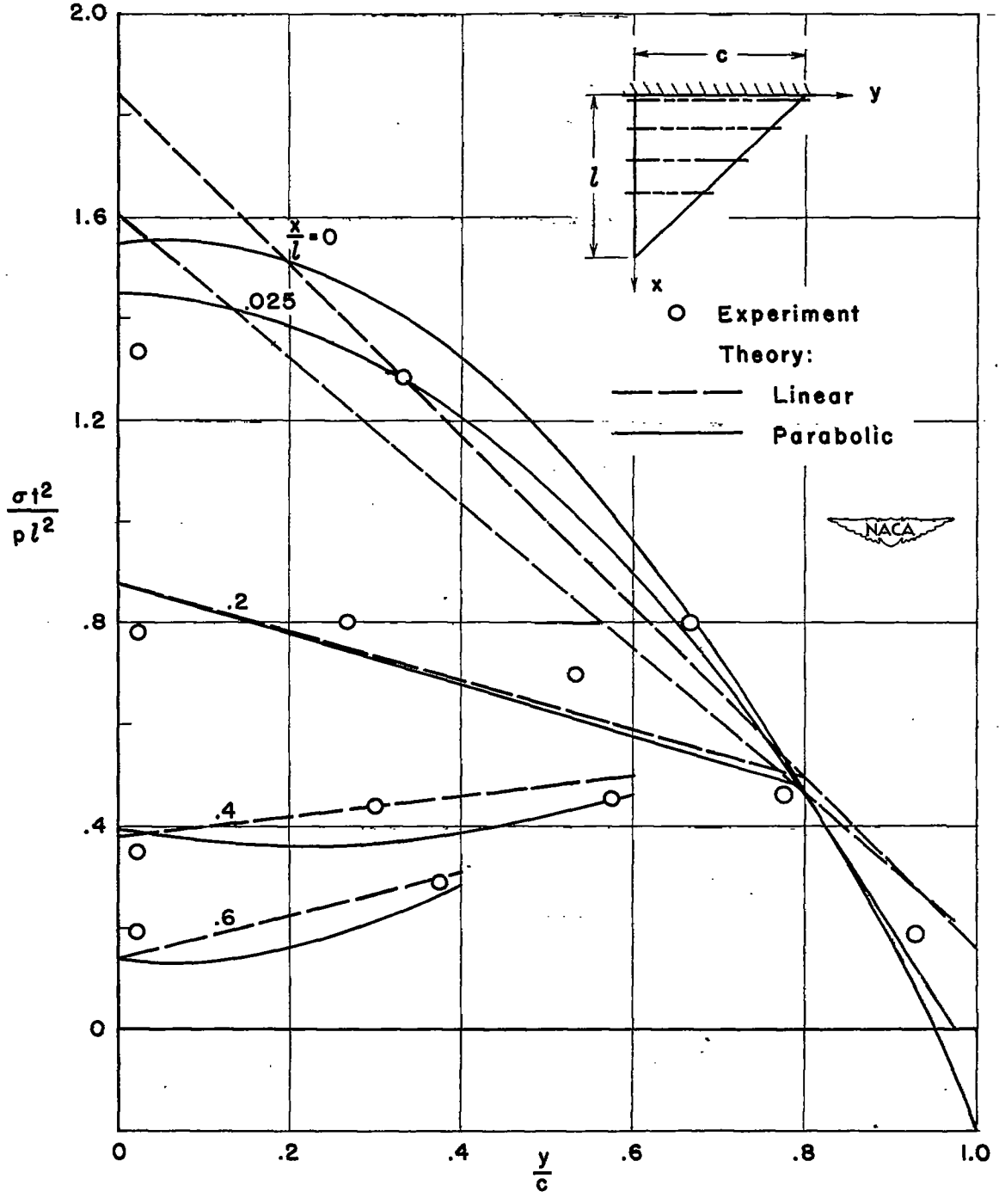

Figure 5.- Maximum principal stresses in a 45° delta plate of uniform thickness under uniform load.

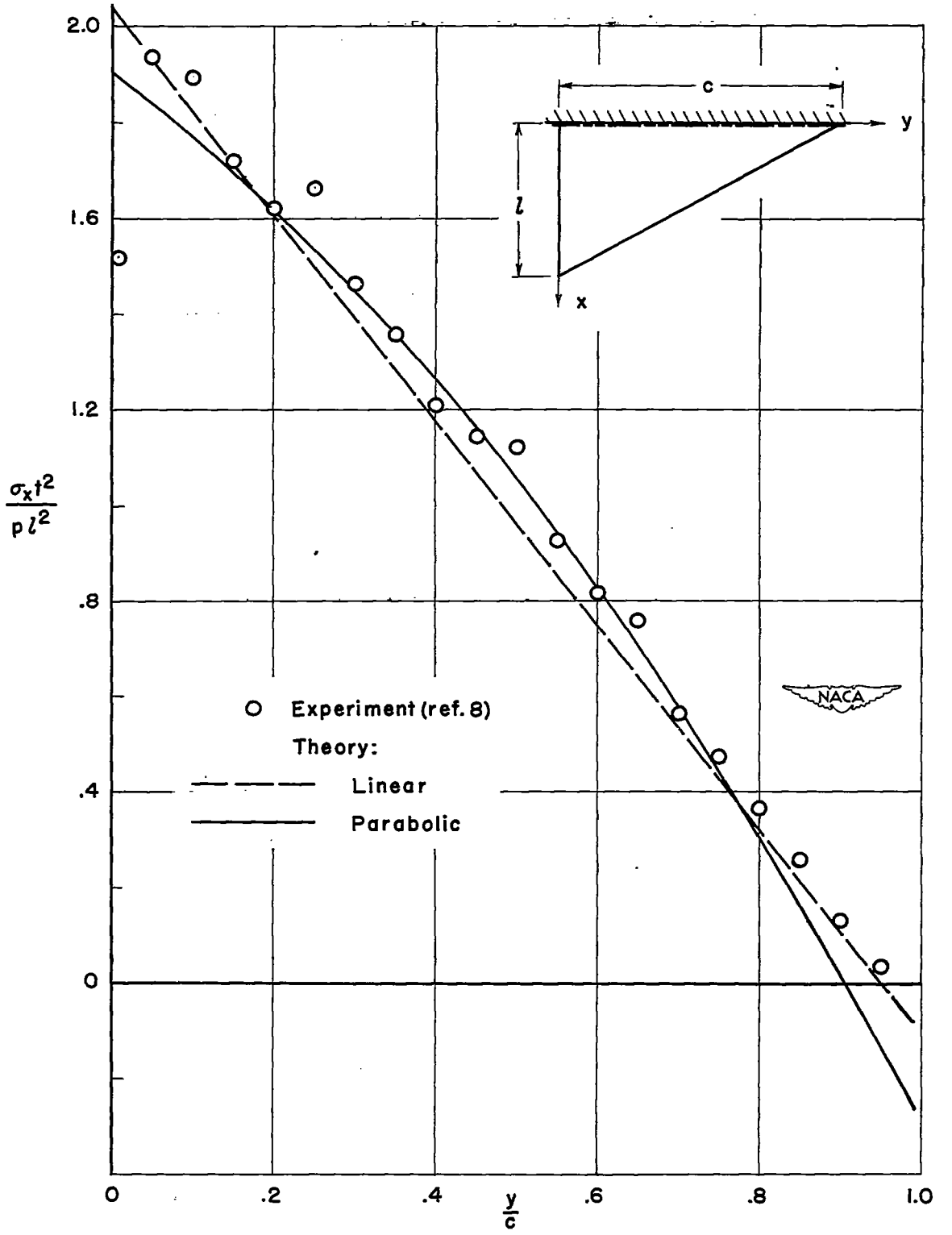

Figure 6.- Normal-stress distribution near the root $\left(\text{at } \frac{x}{l} = 0.0087\right)$ of a 60° delta plate of uniform thickness under uniform load.

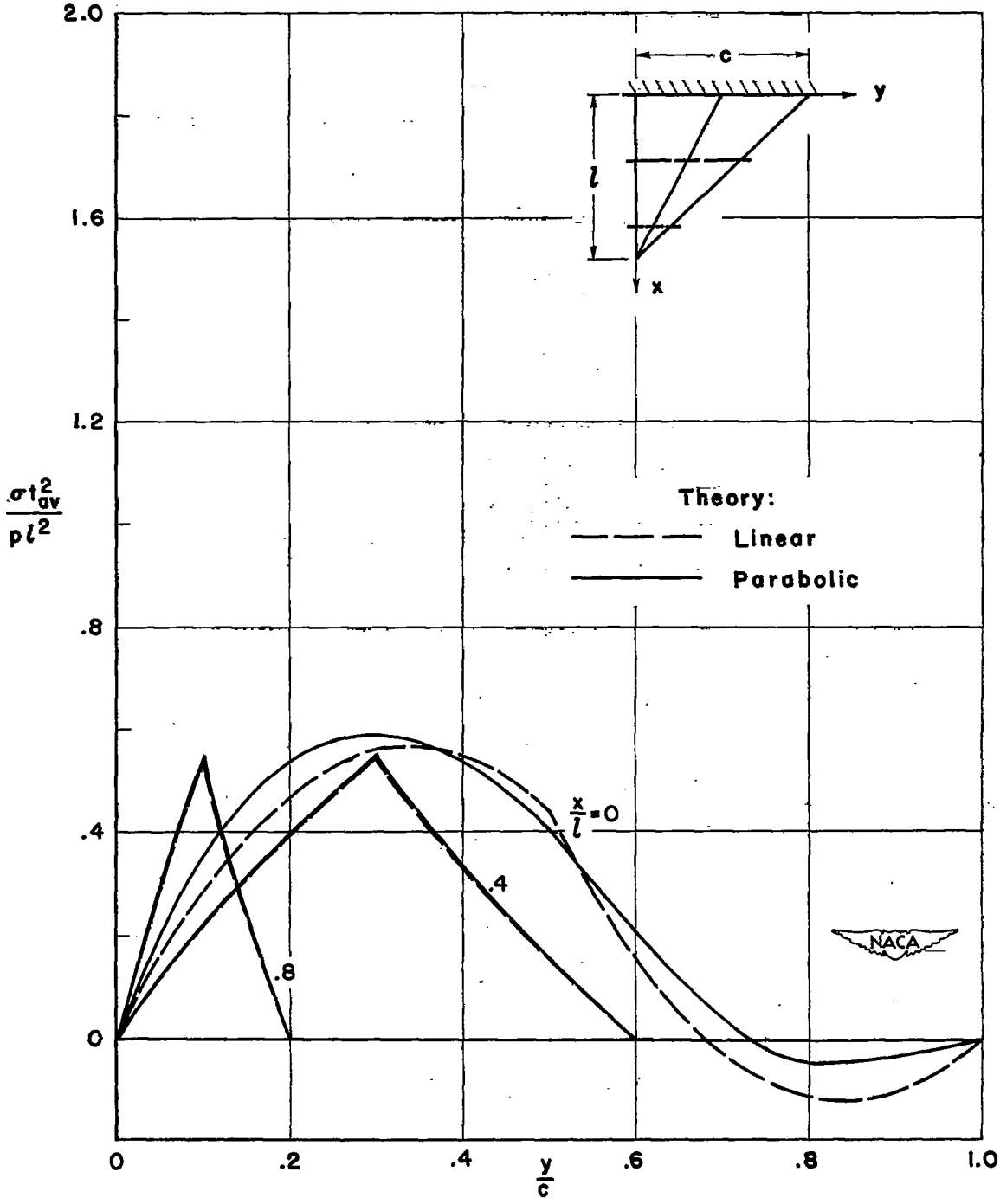

Figure 7.- Maximum principal stress in a 45° delta plate of diamond chordwise cross section and constant thickness ratio under uniform load.

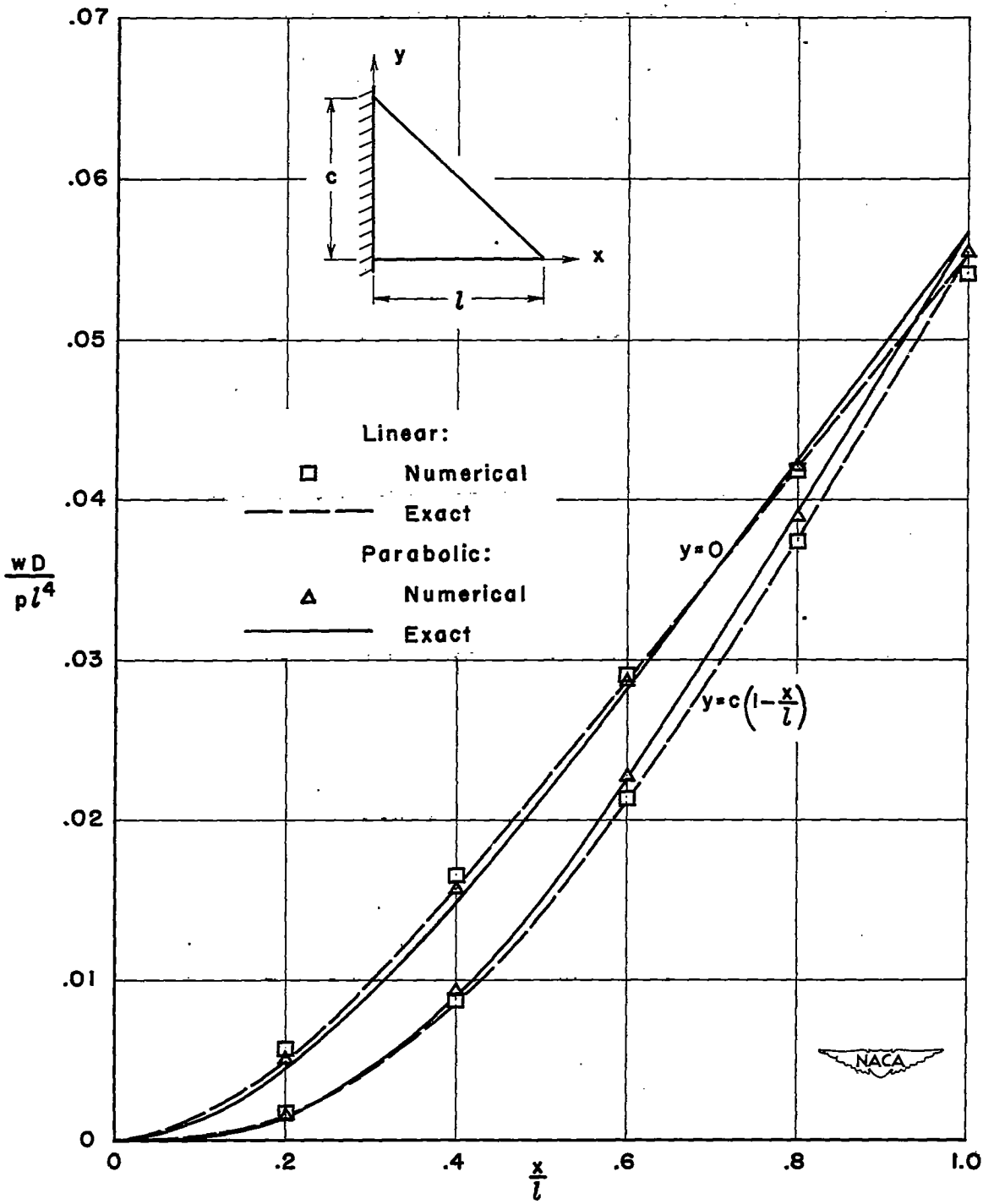

Figure 8.- Numerical and exact solutions of the differential equations for the deflections of the free edges of a 45° delta plate of uniform thickness under uniform load.

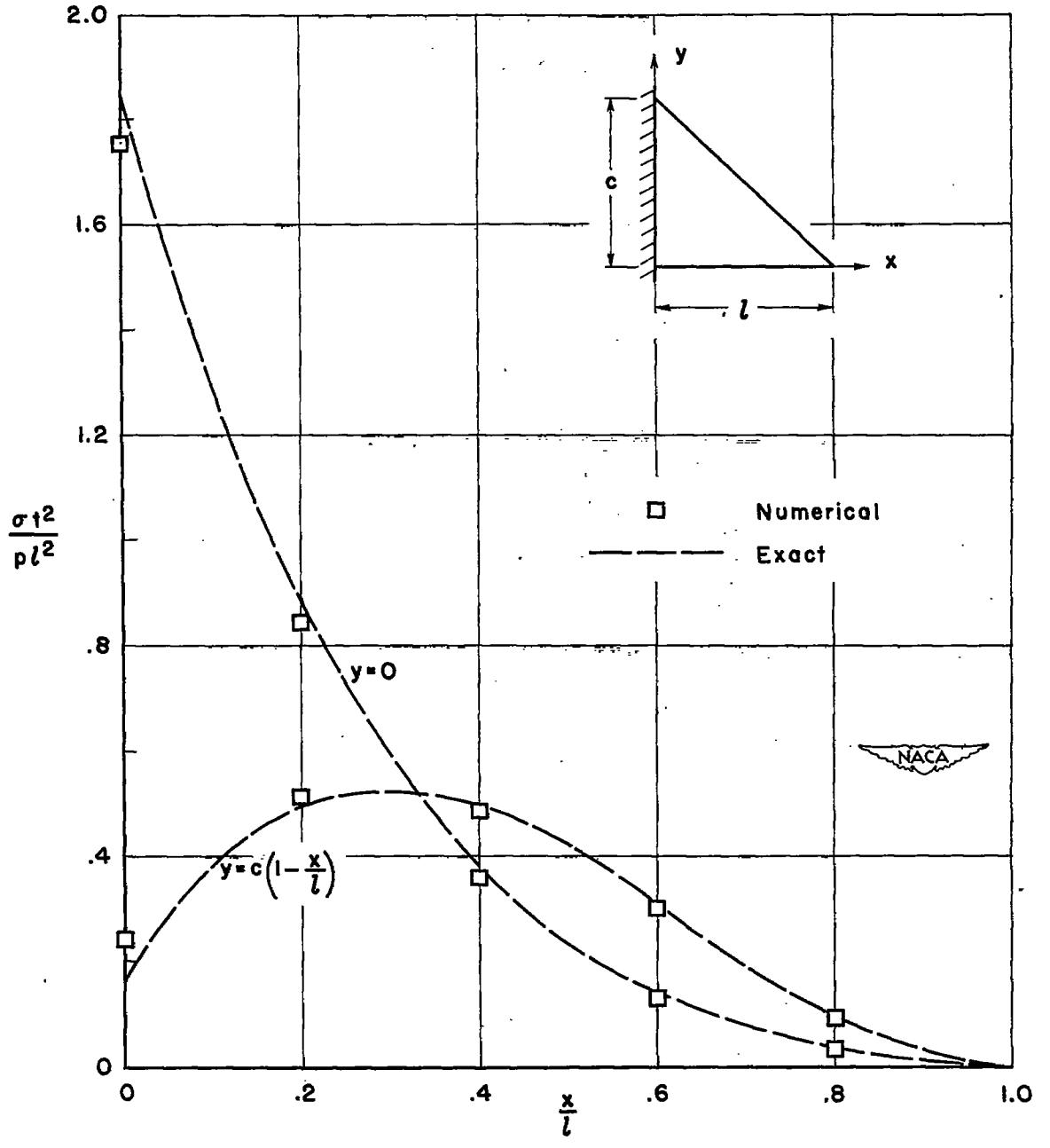

Figure 9.- Numerical and exact solutions of the differential equations (obtained by assuming linear chordwise deflections) for the maximum principal stresses along the free edges of a 45° delta plate of uniform thickness under uniform load.

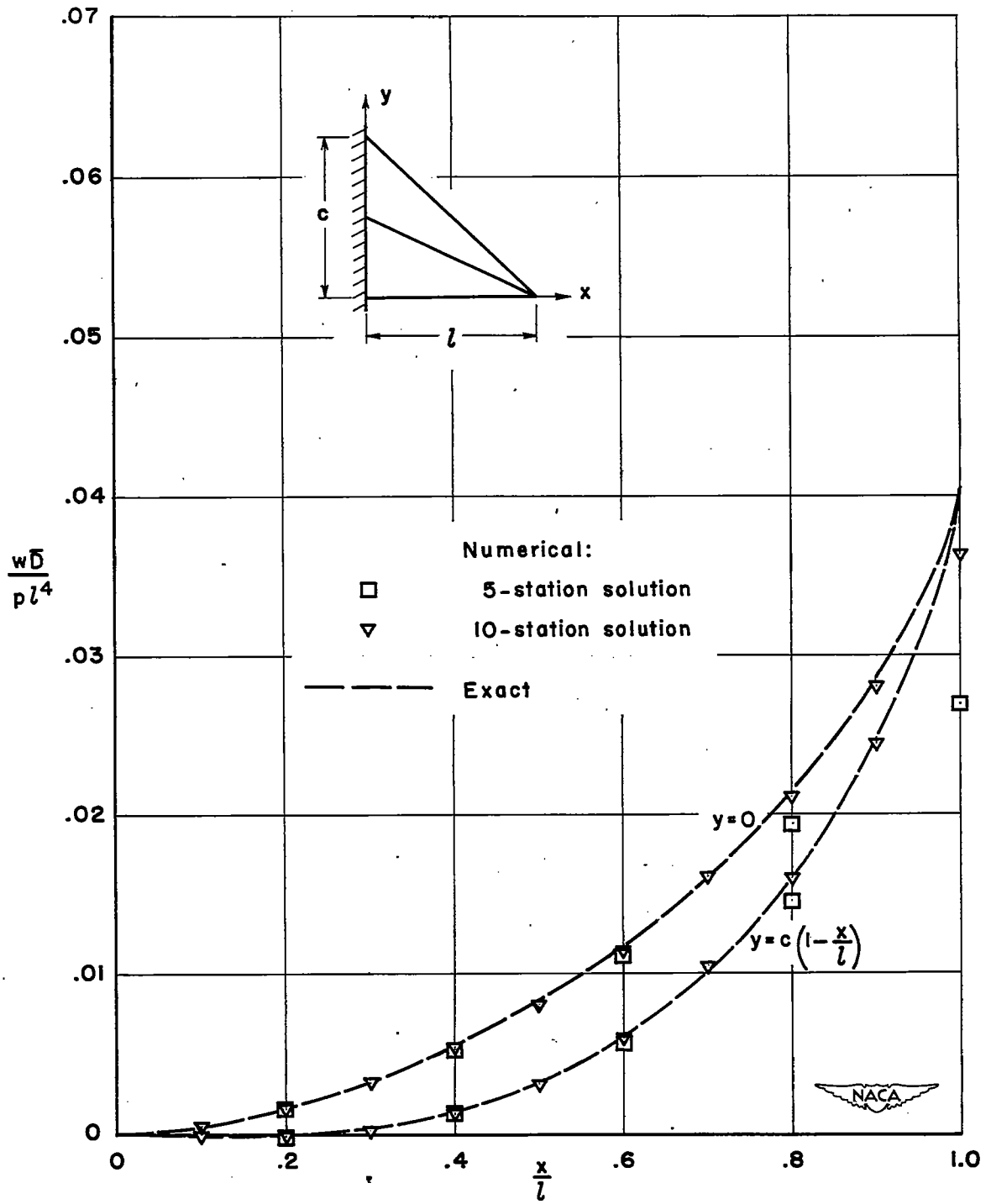

Figure 10.- Numerical and exact solutions of the differential equations (obtained by assuming linear chordwise deflections) for the deflections along the free edges of a 45° delta plate of diamond chordwise cross section and constant thickness ratio under uniform load.

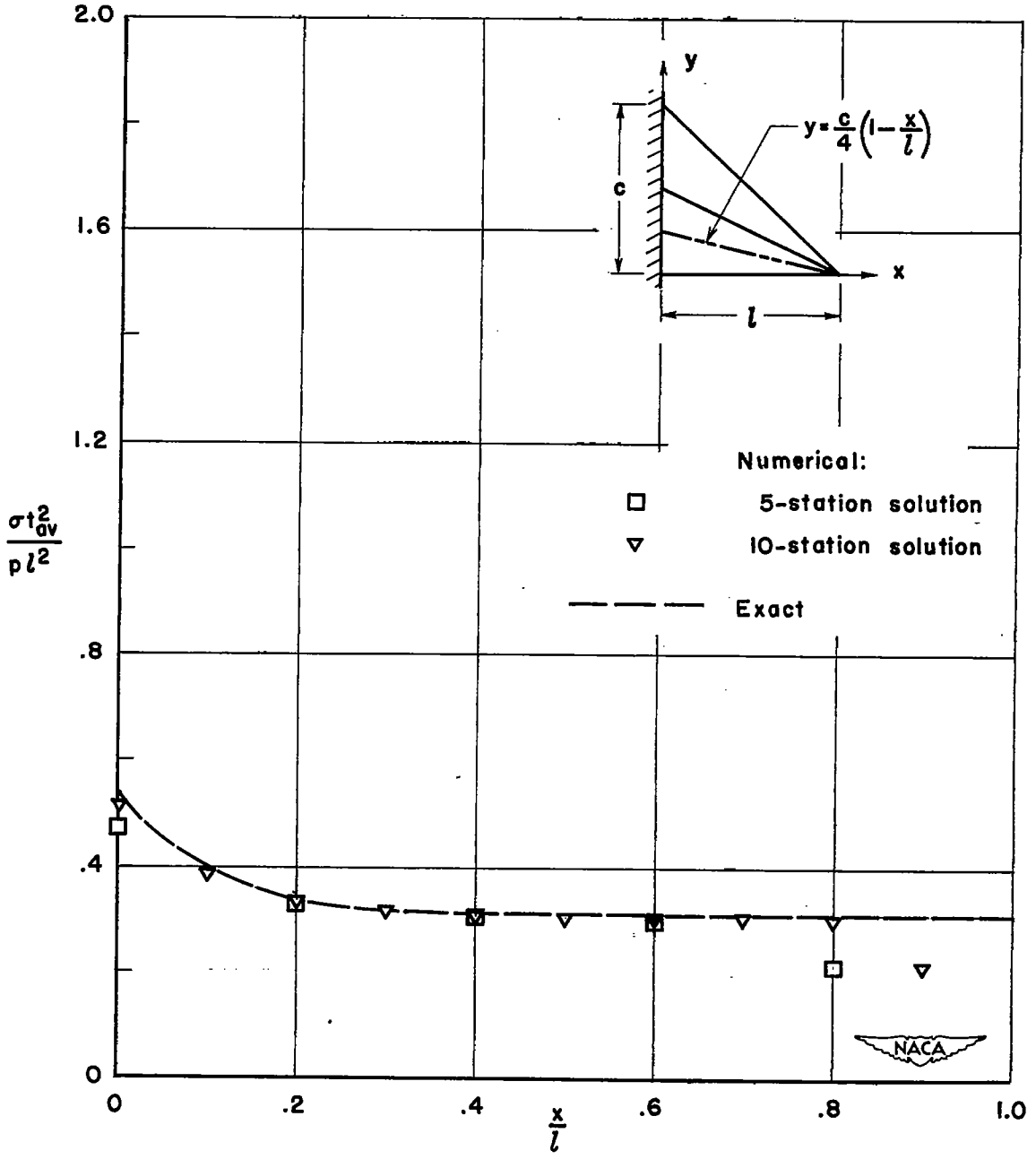

Figure 11.- Numerical and exact solutions of the differential equations (obtained by assuming linear chordwise deflections) for the maximum principal stress along the line $y = \frac{c}{4}\left(1 - \frac{x}{l}\right)$ of a 45° delta plate of diamond chordwise cross section and constant thickness ratio under uniform load.

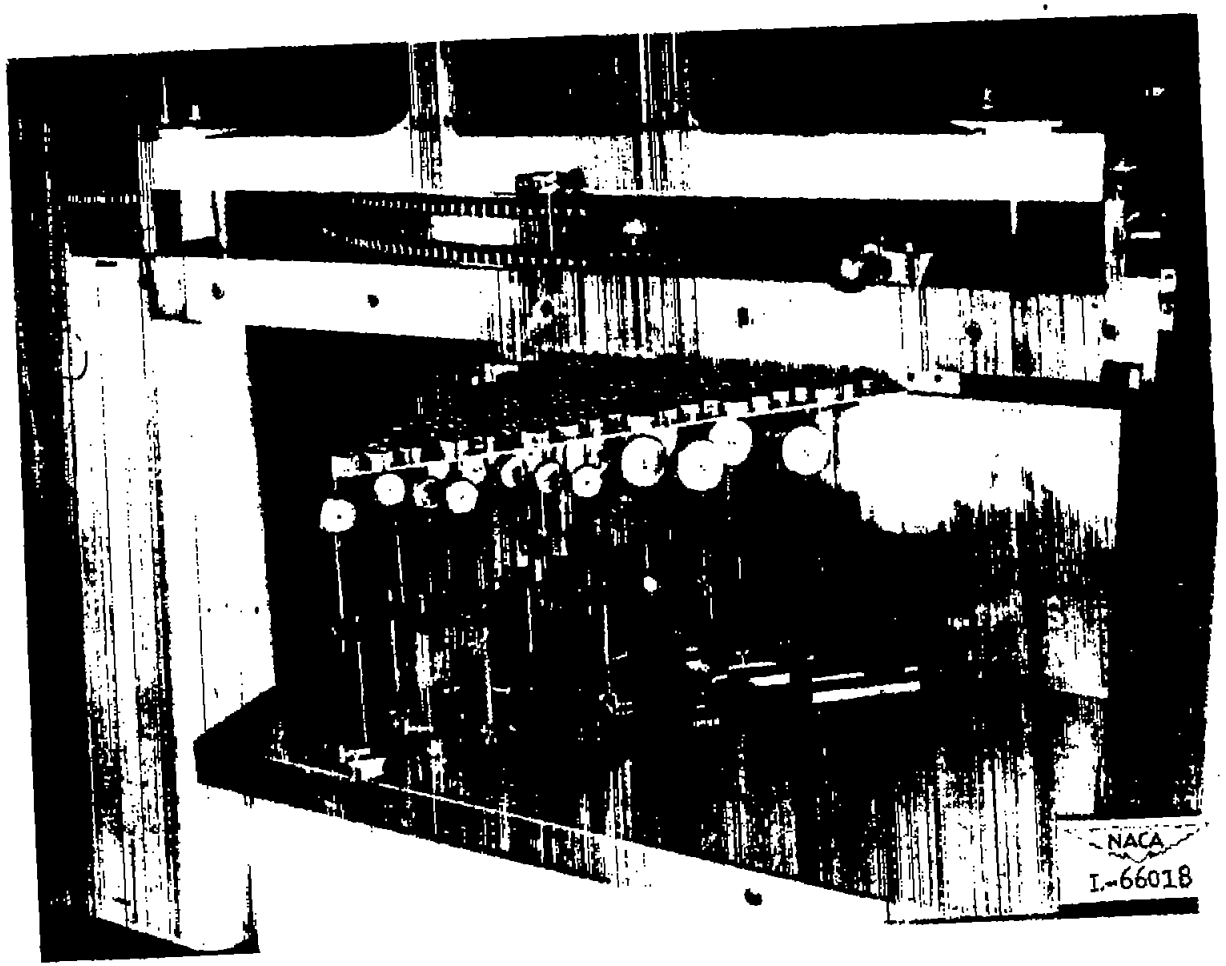

Figure 12.- Deflection test setup of the 45° delta plate under uniform load.